

1 Nutrient transports in the Baltic Sea - results from a 30-year 2 physical-biogeochemical reanalysis

3

4 Ye Liu¹, H.E. Markus Meier^{2,1}, Kari Eilola¹

5 ¹Swedish Meteorological and Hydrological Institute, Norrköping, Sweden

6 ²Leibniz Institute for Baltic Sea Research Warnemünde, Rostock, Germany

7 *Correspondence to:* Ye Liu (ye.liu@smhi.se)

8 **Abstract.** Long-term oxygen and nutrient transports in the Baltic Sea are reconstructed using the Swedish
9 Coastal and Ocean Biogeochemical model (SCOBi) coupled to the Rossby Centre Ocean model (RCO). Two
10 simulations with and without data assimilation covering the period 1970–1999 are carried out. Here, the “weakly
11 coupled” scheme with the Ensemble Optimal Interpolation (EnOI) method is adopted to assimilate observed
12 profiles in the reanalysis system. The reanalysis shows considerable improvement in the simulation of both
13 oxygen and nutrient concentrations relative to the free run. Further, the results suggest that the assimilation of
14 biogeochemical observations has a significant effect on the simulation of the oxygen dependent dynamics of
15 biogeochemical cycles. From the reanalysis, nutrient transports between sub-basins, between the coastal zone and
16 the open sea, and across latitudinal and longitudinal cross sections, are calculated. Further, the spatial
17 distributions of regions with nutrient import or export are examined. Our results emphasize the important role of
18 the Baltic proper for the entire Baltic Sea, with large net transport (export minus import) of nutrients from the
19 Baltic proper into the surrounding sub-basins (except the net phosphorus import from the Gulf of Riga and the net
20 nitrogen import from the Gulf of Riga and Danish Straits). In agreement with previous studies, we found that the
21 Bothnian Sea imports large amounts of phosphorus from the Baltic proper that are retained in this sub-basin. For
22 the calculation of sub-basin budgets, it is crucial where the lateral borders of the sub-basins are located, because
23 net transports may change sign with the location of the border. Although the overall transport patterns resemble
24 the results of previous studies, our calculated estimates differ in detail considerably.

25 **Keywords:** reanalysis; data assimilation; numerical modelling; Baltic Sea; biogeochemical transports; nutrient
26 budgets

27 **1 Introduction**

28 The water exchange between the Baltic Sea and the North Sea is restricted by the narrows and sills in the Danish
29 transition zone (Fig. 1). The hydrography of the Baltic Sea also depends on freshwater from rivers, which causes
30 large salinity gradients between the surface layer and the saltier bottom layer, and between the northern sub-
31 basins and the entrance area (e.g. Meier and Kauker, 2003). The low-saline outflowing surface water is separated
32 from high-saline inflowing bottom water by a transition layer, the halocline. The bottom water in the deep sub-
33 basins is ventilated mainly by so-called Major Baltic Inflows (MBIs) (Matthäus and Franck, 1992; Fischer and
34 Matthäus, 1996). MBIs can significantly affect biogeochemical processes in the deep basins because of the
35 inflow of large volumes of saline and oxygen-rich water into the Baltic Sea (e.g. Conley et al., 2009; Savchuk,
36 2010). In the Baltic Sea, the density stratification and long water residence time hamper the ventilation of deep
37 waters. As a result, oxygen deficiency is a common feature. Additionally, nutrient loads from agriculture and
38 other human activities of the large population in the catchment area increased nutrient concentrations in the water
39 column. Actually, eutrophication has become a large environmental problem in the Baltic Sea in recent decades
40 (e.g. Boesch et al., 2008; Pawlak et al., 2009; Wulff et al., 2001; Andersen et al., 2015). Therefore, accurate
41 estimates of the ecological state and nutrient and water exchange between sub-basins and between the coastal
42 zone and the open sea are of particular importance in managing the marine environment system.

43
44 On one hand, the estimation of biogeochemical processes, ecological state and nutrient exchange may rely on
45 coupled marine ecosystem-circulation models (e.g. Neumann et al., 2002; Eilola et al., 2009; 2011; Almroth-
46 Rosell et al., 2011; 2015; Maar et al., 2011; Daewel and Schrum, 2013). However, addressing biogeochemical
47 cycles is a challenging task due to the complexity of the system. Obviously, there are large uncertainties in
48 marine ecological simulations (e.g. Eilola et al., 2011). In contrast to the modelling of the physics of the

49 atmosphere or ocean, where a basic description of the motion is provided by conservation equations, there is no
50 basic set of equations that describe the marine ecosystem. Many biogeochemical processes are still poorly known
51 and their uncertainties are difficult to quantify accurately. These potential sources of errors limit the applicability
52 of the models both in forecasting and reanalysis. Further, imperfect initial conditions and model forcing also
53 cause biases in the simulation results.

54

55 On the other hand, estimating nutrient budgets and transports between sub-basins may directly rely on
56 observations and basin integrated budget models (Savchuk, 2005). The estimation accuracy depends on the
57 spatial and temporal coverage of the measurements and the locations of borders between sub-basins. Although
58 the data coverage in the Baltic Sea has gradually increased over time, the lack of observations still makes it
59 difficult to estimate reliable biogeochemical cycles. Today, the availability of satellite sensor data like ocean
60 color data from the OCTS (Ocean Color and Temperature Sensor) and from the SeaWiFS (Sea-Viewing Wide
61 Field-of-View Sensor) has provided the best spatial coverage of measurements. However, these sensors only give
62 an estimate of a few biogeochemical parameters at the surface of the marine ecosystem, and not the state of the
63 entire marine ecosystem in the water column. Continuous observations of the deep ocean are only possible with
64 in situ sensors, which have been deployed at only a limited number of stations (Claustre et al., 2010).

65

66 Given the coverage of observations and model deficiencies, we decided to perform a reanalysis based upon a
67 high-resolution, coupled physical-biogeochemical model to estimate the physical and biogeochemical state of the
68 Baltic Sea. For this purpose, data assimilation continuously updates the model variables at the locations of the
69 observations and in their neighborhood. Integration in time of the prognostic model equations allows the spread
70 of the information from the observations within the model domain.

71

72 The assimilation of data into coupled physical-biogeochemical models is confronted by various theoretical
73 and practical challenges. For example, the response of the three-dimensional biogeochemical model to external
74 forcing caused by the physical model is highly non-linear. Further, it is difficult to use the biological
75 observational information to reduce biases in the simulation of ocean physics which has an impact on modeled
76 biogeochemistry (Beal et al., 2010). Besides, data assimilation as used in this study does not conserve mass,
77 momentum and energy. Therefore, a reanalysis with data assimilation can never be dynamically fully consistent.

79 Nevertheless, the use of data assimilation complementing ecosystem modeling efforts has gained widespread
80 attention (e.g. Hoteit et al., 2003; Allen et al., 2003; Natvik and Evensen, 2003; Hoteit et al., 2005; Triantafyllou
81 et al., 2007; While et al., 2012; Triantafyllou et al., 2013; Teruzzi et al., 2014). Data assimilation into ecosystem
82 models has focused both on parameter optimization and on state and flux estimations (Gregg et al, 2009). A
83 comprehensive review of biological data assimilation experiments can be found in Gregg et al. (2009).

84

85 In the Baltic Sea, the biogeochemical data assimilation has started to become a research focus. For example,
86 Liu et al. (2014) used the Ensemble Optimal Interpolation (EnOI) method to improve the multi-annual, high-
87 resolution modelling of biogeochemical dynamics in the Baltic Sea. Fu (2016) analyzed the response of a coupled
88 physical-biogeochemical model to the improved hydrodynamics in the Baltic Sea. Recently, several data
89 assimilation studies have focused on the historical reanalysis of salinity and temperature in the Baltic Sea (e.g. Fu
90 et al., 2012; Liu et al., 2013; 2014). Reanalysis has helped enormously in making the historical record of
91 observed ocean parameters more homogeneous and useful for many purposes. For instance, ocean reanalysis data
92 have been applied in research on ocean climate variability as well as on the variability of biogeochemistry and
93 ecosystems (e.g. Bengtsson et al., 2004; Carton et al., 2005; Friedrichs et al., 2006). Ocean reanalysis can also be
94 used for the validation of a wide range of model results (e.g. Fontana et al., 2013). For instance, the ocean mean
95 state and circulation can be calculated from reanalysis results to evaluate regional climate ocean models (e.g.
96 Meier et al., 2012). Moreover, reanalysis in the ocean is beneficial to the identification and correction of
97 deficiencies in the observational records, as well as filling the gaps in observations. Regional and local model
98 studies may use reanalysis results as initial and boundary conditions. A good reanalysis of biogeochemical state
99 variables can dynamically describe indicators of eutrophication such as the long-term development of water
100 nutrient pools.

101

102 The present paper focuses on the assimilation of profiles of temperature, salinity, nutrients and oxygen in the
103 Baltic Sea following Liu et al. (2014). We aim to reproducing the ocean biogeochemical state with the help of
104 information from both observations and a coupled physical-biogeochemical model for the period 1970-1999.
105 Since 1970 the data coverage in the Baltic Sea is satisfactory. The results of the reanalysis are supposed to be
106 used to estimate the water quality and ecological state with high spatial and temporal resolution in regions and

107 during periods when no measurements are available. Further, nutrient transports across selected cross-sections or
108 between vertical layers are calculated with high resolution and accuracy taking the complete dynamics of
109 primitive equation models into account. This information cannot be obtained from either observations alone or
110 from model results without data assimilation because the latter might have large biases in both space and time.
111 We assess the nutrient budgets of the water column as well as of the nutrient exchanges between sub-basins and
112 between the coastal zone and the open sea. The calculated budgets are compared to the results of other studies to
113 evaluate our results. Hereby, we follow studies of other regions applying data assimilation for a biogeochemical
114 reanalysis on long-term scale (Fontana et al., 2013; Ciavetta et al., 2016).

115

116 This paper is organized as follows. The physical and biogeochemical models are described in Section 2. Then
117 the observational data set and the method of the reanalysis are introduced in Section 3 and 4, respectively. The
118 experiment results, including comparisons with observations, are presented in Section 5. Finally, in Section 6 and
119 7, discussion and conclusions finalize the paper.

120 **2 Models**

121 The RCO (Rossby Centre Ocean) model is a Bryan–Cox–Semtner primitive equation circulation model with a
122 free surface (Killworth et al., 1991). Its open boundary conditions are implemented in the northern Kattegat,
123 based on prescribed sea level elevation at the lateral boundary (Stevens, 1991). An Orlanski radiation condition
124 (Orlanski, 1976) is used to address the case of outflow, and the temperature and salinity variables are nudged
125 toward climatologically annual mean profiles to deal with inflows (Meier et al., 2003). A Hibler-type dynamic–
126 thermodynamic sea ice model (Hibler, 1979) with elastic–viscous–plastic rheology (Hunke and Dukowicz, 1997)
127 and a two-equation turbulence closure scheme of the k – ε type with flux boundary conditions (Meier, 2001) have
128 been embedded into RCO. The deep-water mixing is assumed inversely proportional to the Brunt–Väisälä
129 frequency, with the proportionality factor based on dissipation measurements in the Eastern Gotland Basin (Lass
130 et al., 2003). In its present version, RCO is used with a horizontal resolution of 2 nautical miles (3.7 km) and 83
131 vertical levels, with layer thicknesses of 3 m. RCO allows direct communication between bottom boxes of the
132 step-like topography (Beckmann and Döscher, 1997). A flux-corrected, monotonicity-preserving transport (FCT)

133 scheme is applied in RCO (Gerdes et al., 1991). RCO has no explicit horizontal diffusion. For further details of
134 the model setup, the reader is referred to Meier et al. (2003) and Meier (2007).

135
136 The biogeochemical model called SCOBI (Swedish Coastal and Ocean Biogeochemical model) has been
137 developed to study the biogeochemical nutrient cycling in the Baltic Sea (Marmefelt et al., 1999; Eilola et al.,
138 2009; Almroth-Rosell et al., 2011; 2015). This model handles biological and ecological processes in the sea as
139 well as sediment nutrient dynamics. SCOBI is coupled to RCO (e.g. Eilola et al., 2012; 2013; 2014). With the
140 help of a simplified wave model, resuspension of organic matter is calculated from the wave and current-induced
141 shear stresses (Almroth-Rosell et al., 2011). SCOBI has a constant carbon (C) to chlorophyll (Chl) ratio $C:Chl =$
142 $50 \text{ (mg C (mg Chl)}^{-1})$, and the production of phytoplankton assimilates carbon (C), nitrogen (N) and phosphorus
143 (P) according to the Redfield molar ratio ($C:N:P = 106:16:1$) (Eilola et al., 2009). The molar ratio of a complete
144 oxidation of the remineralized nutrients is $O_2:C = 138$. For further details of the SCOBI model, the reader is
145 referred to Eilola et al. (2009, 2011) and Almroth-Rosell et al. (2011).

146
147 RCO-SCOBI is forced by atmospheric forcing data calculated from regionalized ERA-40 data using the
148 regional Rossby Centre Atmosphere (RCA) model (Samuelsson et al., 2011). The horizontal resolution of RCA is
149 25 km. A bias correction method following Meier et al. (2011) is applied to the wind speed. Monthly mean river
150 runoff observations (Bergström and Carlsson, 1994) are used for the hydrological forcing. Monthly nutrient loads
151 are calculated from historical data (Savchuk et al., 2012).

152 **3 Observations**

153 The Baltic coastal shelf observation systems have been largely improved by the joint efforts of the countries
154 surrounding the Baltic Sea. For example, the International Council for the Exploration of the Sea (ICES)
155 (<http://www.ices.dk>) and the Swedish Oceanographic Data Centre (SHARK) (<http://sharkweb.smhi.se>) are
156 collecting the observations with the aim to monitor the Baltic Sea. Furthermore, the Baltic Sea Operational
157 Oceanographic System (BOOS) (<http://www.boos.org/>) is providing near real-time observations and the publicly
158 available database BED (Baltic Environmental Database, <http://nest.su.se/bed>) of the Baltic Nest Institute (BNI)
159 (<http://www.balticnest.org>) store physical and environmental data from BNI partner institutes (see

160 http://nest.su.se/bed/hydro_chem.shtml). Also the data of SHARK have been stored in BED. As a result, a
161 comprehensive data set is collected for the Baltic Sea region. The assimilated observations in this study comprise
162 both physical (temperature and salinity) and biogeochemical variables (oxygen, nitrate, phosphate and
163 ammonium) from the SHARK database. Before assimilation, the data were quality controlled. These controls
164 include checks of location and duplication, and examination of differences between forecasts and observations. A
165 profile was eliminated from the assimilation procedure when the station was located on land defined by the RCO
166 bathymetry. We also removed observations when the difference between model forecasting field and
167 observations exceeds the given standard maximum deviation (for example 4.0 mL L⁻¹ for oxygen concentration).
168 We used an average of the observations in the same layer when there was more than one observation per layer.
169 These observations cover almost the whole Baltic Sea including Kattegat and the Danish Straits. Figure 2 shows
170 the number of biogeochemical observation profiles in different sub-basins, and the temporal distribution of these
171 biogeochemical observations. The number of observations is inhomogeneous in both temporal and spatial
172 distribution over the period from 1970 to 1999. There are relatively more observations in the Baltic proper than in
173 other sub-basins. In the Gulf of Riga, a minimum number of observation profiles (30 for oxygen, 30 for
174 phosphate, 28 for nitrate and 28 for ammonium) is found. Obviously, the number of observations during the
175 period of 1988-1994 is higher than that during other periods. Further, there are generally less observations from
176 1981-1983 than during other periods. The maximum number of observation profiles occurred in 1991 for oxygen
177 (1,844), phosphate (1,728) and nitrate (1,758). However, the number of ammonium observation profiles has a
178 maximum value of 1,222 in 1992. Moreover, compared to other variables the numbers of oxygen and ammonium
179 observations are largest and smallest, respectively. These observations from SHARK and BED are used to
180 validate the model and assimilation results.

181

182 The simulated spatial variations of the late winter surface layer nutrient concentrations are compared with the
183 spatial variations reconstructed from BED with the Data Assimilation System (DAS) by Sokolov et al. (1997).
184 Due to insufficient historical data coverage the average March fields were computed for time period (1995–2005)
185 from over 3600 oceanographic stations found in BED. Also nutrient pools of dissolved inorganic nitrogen (DIN)
186 and phosphorus (DIP) calculated with DAS (see Savchuk, 2010) are compared with the results of this study. See
187 Eilola et al. (2011) for more details about the data handling by DAS.

188 4 Methodology and Experimental Setup

189 Here we briefly describe the configuration of the data assimilation system of this study. We focus on the state
 190 estimation via EnOI. The distribution of stochastic errors are assumed to be Gaussian and non-biased. EnOI
 191 estimates an 'optimal' oceanic state at a given time using observations, the numerical model and assumptions on
 192 their respective bias distribution. The relationship between them can be expressed as following:

$$193 \quad \boldsymbol{\psi}^a = \boldsymbol{\psi}^f + \mathbf{K}(d - H\boldsymbol{\psi}^f) \quad (1),$$

$$194 \quad \mathbf{K} = \mathbf{P}^f H^T (H\mathbf{P}^f H^T + (N-1)\mathbf{R})^{-1} \quad (2).$$

195 Where $d \in \mathfrak{R}^m$ is the vector of observations with m being the number of observations. $\boldsymbol{\psi} \in \mathfrak{R}^n$ is the n
 196 dimensional model state vector which includes the sea level anomaly, temperature, salinity, oxygen, phosphate,
 197 ammonium and nitrate. The superscripts a and f refer to ‘‘analysis’’ and ‘‘forecast’’, respectively. $\mathbf{K} \in \mathfrak{R}^{n \times m}$ is
 198 the Kalman gain matrix and H is an operator that maps the model state onto the observation space—often H is
 199 linear interpolation. $d - H\boldsymbol{\psi}^f \in \mathfrak{R}^m$ is the innovation which is calculated in the observation space. $\mathbf{R} \in \mathfrak{R}^{m \times m}$ is
 200 the observation error covariance. N is the number of the ensemble samples. EnOI computes the Background
 201 Error Covariance (BEC) matrix $\mathbf{P} \in \mathfrak{R}^{n \times n}$, which determines how to spread out information from observations in
 202 space and between variables, by the ensemble perturbation matrix $\mathbf{A}' = \mathbf{A} - \bar{\mathbf{A}}$ as follows:

$$203 \quad \mathbf{P} = \frac{\alpha}{N-1} \mathbf{A}'(\mathbf{A}')^T \quad (3).$$

204 Here $\mathbf{A} = (\boldsymbol{\psi}_1, \boldsymbol{\psi}_2, \dots, \boldsymbol{\psi}_N) \in \mathfrak{R}^{n \times N}$ is the sample ensemble and $\bar{\mathbf{A}} = \frac{1}{N} \sum_{i=1}^N \boldsymbol{\psi}_i$ is the sample ensemble mean. The
 205 subscript T denotes the transpose of a matrix and the scaling factor $\alpha \in (0, 1]$ is introduced to tune the variance
 206 of the sample ensemble perturbations to a realistic level in order to capture the variability of model parameters
 207 like temperature and dissolved oxygen, which is dominated by misplacement of mesoscale features and which
 208 varies in location and intensity seasonally. Therefore, we hypothesize that the background errors are proportional
 209 to the model variability on intra-seasonal time scales. We selected the samples from model results of a hindcast
 210 simulation without data assimilation from one and a half month before and after the calendar date of the

211 assimilation time during the period 1964–1968 (Liu et al., 2013). The snapshots during the period 1964-1968
212 have been stored every three days. From every year during the selected period 1964–1968 20 snapshots have
213 been selected. Hence, a total of $N = 100$ model samples are adopted to obtain a quasi-stationary BEC matrix.
214 The analysis by EnOI rely on the sample ensemble because the analysis increment is a linear combination of
215 sample ensemble anomalies. Other, more “sophisticated” sample ensembles could be tested but this is beyond the
216 scope of this study. An adaptive scaling factor was calculated to adapt to the instantaneous forecast error variance
217 before each local analysis (Liu et al., 2013; 2014). Further, localization is used to remove unrealistic long-range
218 correlation with a quasi-Gaussian function and a uniform horizontal correlation scale of 70 km. As a result, the
219 quality of fields obtained by data assimilation is determined by the coverage and quality of observations (She et
220 al., 2007). Moreover, the assimilation frequency or window is another factor to affect the assimilation fields.
221 They are directly related to how many observations are entering the assimilation cycling and how often the model
222 initial condition is adjusted by data assimilation (Liu et al., 2013). Here, we select an assimilation window of
223 three days and the assimilation frequency is once every seven days in the reanalysis experiment. It means that all
224 the observations in three days before and after the assimilation time are selected to yield the “new” initial
225 condition for the following simulation during the current assimilation cycle. When observations become available
226 at a certain time, the 'optimal' state variables are calculated by Equation 1, which are used as new initial
227 conditions for the next simulation cycle.

228

229 Based on the above configuration, two experiments from January 1970 to December 1999 have been carried
230 out. One experiment is a simulation without data assimilation (FREE). The other simulation is constrained by
231 observations using the “weakly coupled” assimilation scheme based upon the EnOI method following Liu et al.
232 (2014) which was briefly described above (REANA). Both simulations, FREE and REANA, are initialized for
233 January 1970. The initial conditions are taken from an earlier run with RCO-SCOBI. The observation error in
234 REANA is defined according to Liu et al. (2014). However, in Liu et al. (2014), only a shorter assimilation
235 experiment for a 10-year period is presented, and so far the reliability of the assimilation scheme in multi-decadal
236 simulations has not been shown. Following Liu et al. (2014), our REANA experiment assimilated both physical
237 and biogeochemical observations. In this study, we focus mainly on nutrient transports derived from the
238 reanalysis.

239

240 To assess the results with (REANA) and without (FREE) data assimilation, the overall monthly mean RMSDs
 241 (root mean square differences) of oxygen, nitrate, phosphate and ammonium were calculated relative to
 242 observations during the whole integration period. The overall monthly mean RMSD is calculated by the
 243 following formula:

$$244 \quad RMSD = \frac{1}{N_j} \sum_{j=1}^{N_j} \sqrt{\frac{1}{N_t} \sum_{i=1}^{N_t} (\epsilon_t^i)^2} \quad (4),$$

245 where N_t is the number of the observations at assimilation time t and N_j is the number of days of one month
 246 for one field for the entire Baltic Sea. $\epsilon_t^i = x_{sim}^i(t) - x_{obs}^i(t)$ represents the difference between model result (x_{sim})
 247 and observation (x_{obs}) at time t and at the i^{th} observation location. We calculated ϵ_t only at the locations of the
 248 observations at the time t , which is calculated by mapping the model field onto the observation space. Here it
 249 should be noted that the RMSDs were calculated before the time of assimilation analysis, and the corresponding
 250 observations were not yet assimilated into RCO-SCOBI (Liu et al., 2014).

251
 252 Based on the reanalyzed simulation, the annual mean DIN and DIP transports as well as DIP persistency are
 253 also calculated. These transports (VA_{Trans}) are vertically integrated from the sea floor to the sea surface at every
 254 horizontal position at every time step of the integration according to:

$$255 \quad VA_{Trans} = \sum_{k=1}^N C_k u_k \Delta z_k \quad (5),$$

where $C_k, u_k, \Delta z_k$ and N are the field concentrations of DIN, DIP or organic phosphorus (OrgP), the current
 velocity vector in horizontal direction, vertical dimensions of a grid cell and the number of wet grid cells in the
 water column, respectively. From the net transport vector field both magnitude and streamlines are calculated.

256 The total nutrient budgets are calculated from the sum of inorganic and organic bioavailable nutrients. The
 257 combined nutrient supplies from land and from the atmosphere have been taken into account. Nitrogen fixation is
 258 not included in the external supplies. The sinks of the nutrient budgets are calculated from the supplies from
 259 land/atmosphere, import/export from other basins and the changes in pelagic nutrient pools during the period
 260 (sink=supply+import-export-pool change). By this definition the nitrogen sink includes nitrogen fixation and

261 denitrification. The nutrient flows for the total budgets are integrated along the selected borders of sub-basins
 262 using Equation 5. Annual nutrient flows are averaged for the period 1970-1999. The total amount of nutrients for
 263 every sub-basin is calculated from the integral of nutrient concentrations from phytoplankton, zooplankton,
 264 detritus and dissolved nutrient times the volume of the sub-basin according to:

$$265 \quad Total = \sum_{i=1}^{N_i} \sum_{j=1}^{N_j} \sum_{k=1}^{N_k} C_{i,j,k} \Delta x_{i,j} \Delta y_{i,j} \Delta z_k \quad (6),$$

where $C_{i,j,k}$, $\Delta x_{i,j}$, $\Delta y_{i,j}$ and Δz_k are the field concentrations (including nutrients from phytoplankton,
 zooplankton, detritus and dissolved nutrients), the horizontal and vertical dimensions of a grid cell, respectively.
 N_i , N_j and N_k are the number of grid cells in horizontal and vertical direction for every sub-basin, respectively.
 Net transports across sections of sub-basins are calculated from the difference between export and import
 (relevant for the results in Sections 5.6 and 5.7).

266 **5 Results**

267 In the following sub-sections, we evaluate the impact of data assimilation on the long-term evolution of biases
 268 (Section 5.1), and on vertical (Section 5.2) and horizontal (Section 5.3) distributions of nutrient concentrations.
 269 For the evaluation of time series of simulated oxygen, nitrate, phosphate and ammonium concentrations, the
 270 reader is referred to Liu et al. (2014, their Figs. 6 and 7). After the evaluation of the assimilation method, we
 271 focus on the analysis of nutrient transports in the Baltic Sea based upon our reanalysis data that we consider to be
 272 the best available data set for such an analysis. In particular, we analyze the horizontal circulation of nutrients
 273 (Section 5.4), the horizontal distribution of nutrient sources and sinks, the nutrient exchange between the coastal
 274 zone and the open sea (Section 5.5), and the nutrient budgets of sub-basins (Section 5.6).

275 **5.1 Temporal evolution of biases and pools**

276 The biases in both FREE and REANA have been calculated relative to observations for dissolved oxygen and
 277 inorganic nutrients using Equation 4 (Fig. 3). Data assimilation has significantly reduced bias of the model
 278 simulation. Generally, the RMSDs of oxygen and nutrient concentrations in REANA are smaller than that of

279 FREE. However, the degree of improvements differs among the variables. The RMSD of oxygen is mostly
280 greater and smaller than 1.0 mL L^{-1} for FREE and REANA, respectively. The mean RMSD of oxygen during this
281 period has been reduced by 59% (from 1.43 to 0.59 mL L^{-1}). Similar improvements appear in nitrate and
282 phosphate concentrations. The mean RMSDs of nitrate and phosphate in REANA were reduced by 46% (from
283 2.04 to 1.11 mmol m^{-3}) and 78% (from 1.05 to 0.23 mmol m^{-3}) relative to that in FREE, respectively.
284 Furthermore, the variability of RMSD of phosphate in FREE is large during the first 10 years, and decreases
285 afterwards with time. However, the data assimilation cannot always improve the model results. For instance,
286 although the mean RMSD of ammonium is reduced by 45% (from 1.15 to 0.63 mmol m^{-3}), the ammonium
287 concentrations in REANA become worse relative to those in FREE during some months. An example appears in
288 February 1975 when the RMSD of the ammonium concentrations in REANA (3.07 mmol m^{-3}) is greater than that
289 in FREE (2.75 mmol m^{-3}). These results are similar to the findings by Liu et al. (2014). However, here we show
290 that even the 30-year long assimilation is reliable, and that the RMSD of phosphate concentration decreases even
291 further with data assimilation continuing for more than 10 years.

292

293 Further, the annual averaged pelagic pools of simulated DIN and DIP in the Baltic proper are compared to the
294 corresponding pools estimated from the BED data in the Baltic proper (Fig. 4). The maximum annual differences
295 of DIN and DIP pools compared to BED, have been reduced by 57.5% and 72.3%, respectively, from 400 kton
296 and 650 kton in FREE (not shown) to 170 kton and 180 kton in REANA. The remaining differences between
297 REANA and BED may be explained by the methods of integration that differ. BED estimates are based on a
298 limited amount of observations while the model results are based on a large number of grid points with
299 dynamically varying state variables. A similar result for hypoxic area was found by Väli et al. (2013). They
300 showed with the help of model results which were sampled at the same times and locations of the observations
301 that the applied interpolation algorithm underestimated hypoxic area by about 40%.

302 **5.2 Mean seasonal cycle of nutrients**

303 The long-term average seasonal cycles of temperature and inorganic nutrients at monitoring station BY15 at
304 Gotland Deep (for the location, see Fig. 1) give a hint of how data assimilation improves simulated nutrient
305 dynamics in the Baltic proper (Fig. 5). The surface layer temperature and stratification show rapid increase in

306 April to May, with concurrent rapid decrease of nutrient concentrations due to primary production down to 50–60
307 m depths. The cooling and increased vertical mixing in autumn and winter reduce temperatures and bring
308 nutrients from the deeper layers into the surface layers. RCO-SCOB1 captures these variations. However,
309 compared to BED, FREE has obvious biases, such as overestimated temperature stratification around 30–50 m
310 depth from late winter to early spring, higher concentration of nutrients at the 50–60m depth, stronger vertical
311 stratification of nutrient concentrations and less decrease of nutrients in the summer, especially below the
312 thermocline, as well as also in the surface layers for phosphate. One reason for the biases is the vertical
313 displacement of the halocline that is too shallow in RCO (e.g. Fig. 4 in Liu et al., 2014). The causes for the model
314 bias in nutrient depletion below the summer thermocline are not known, but possible reasons are discussed by
315 Eilola et al. (2011). These biases are significantly reduced in the reanalysis which provides an improved
316 description of vertical distributions of nutrients in the layers above the halocline.

317 **5.3 Spatial variations of late winter nutrient concentrations**

318 The average March concentrations (1970-1999) of DIP and DIN in the upper layers (0–10m), as well as their
319 ratio (DIN:DIP), were calculated (Fig. 6). Due to insufficient historical data the corresponding BED maps
320 describe the averages for the period 1995–2005 as a basis for model to data comparison. In BED results the
321 highest concentration of DIP occurs in the Gulf of Riga and the Gulf of Finland. Relatively high concentrations
322 of DIP are found in the entire Gotland Basin. The DIP concentrations in the Bothnian Sea and Bothnian Bay are
323 obviously lower than in other regions. Generally, the DIP in FREE has been largely overestimated in all regions
324 relative to BED, especially in the Baltic proper. Further, in BED high concentrations of DIN occur in coastal
325 waters close to the river mouths of the major rivers in the southern Baltic proper. DIN concentrations in the Gulf
326 of Finland and in the Gulf of Riga are also high, and cover large areas of these gulfs. Unlike the BED data, the
327 DIN in FREE has high concentrations also in the entire southern and eastern coastal zones of the Baltic proper.
328 As a result, FREE shows a gradient in DIN concentrations between the coastal zone and the open sea in the entire
329 southern Baltic proper. The DIN and DIP patterns result in high and low DIN:DIP ratios in the Bothnian Bay and
330 Baltic proper, respectively. The highest DIN:DIP ratios are found in the Bothnian Bay in BED and in the Gulf of
331 Riga in FREE. FREE has captured this large-scale pattern, but there are substantial regional differences. By the
332 constraints of the observation information, REANA has improved the spatial distributions of DIN and DIP

333 significantly compared to BED. In particular, DIP concentrations in REANA are much closer to the interpolated
334 BED observations.

335

336 **5.4 Mean horizontal circulation of nutrients**

337 Nutrient transport directly affects the biogeochemical cycles and the eutrophication of the Baltic Sea. The
338 persistency of vertically integrated transports (Fig. 7) is defined, for instance, by Eilola et al. (2012). One should
339 note that the results by Eilola et al. (2012) are based upon 30-year averages for the control period 1978-2007 of a
340 downscaled climate scenario from a global circulation model. Similar calculations of transports will therefore be
341 briefly presented in the present study, since the hindcast period is better represented when the model is forced by
342 the assimilated atmospheric (ERA-40) and Baltic Sea data (REANA). DIP has the largest transports in the central
343 parts of the Baltic proper, with high persistency because the volume transports are generally larger in deeper
344 rather than in shallower areas. In the Bornholm Basin and the eastern parts of the central Baltic proper, cyclonic
345 circulation patterns are found. In the western parts of the central Baltic proper, southward transports prevail.
346 Relatively large magnitudes of transports of DIP are also found in the northwestern Gotland Basin, in the
347 southern Bornholm Basin, and through the Slupsk Channel connecting Bornholm Basin and Gotland Basin.
348 Similar transport patterns are also found for DIN, OrgP and OrgN (not shown). Compared to Eilola et al. (2012),
349 DIN, DIP, OrgP and OrgN transports and their persistency are larger, although the overall patterns are similar.
350 For example, in Eilola et al. (2012, their Fig. 1), large DIN transports appear in the southern Baltic proper and the
351 Bornholm Basin. Similar differences are also found in both DIP and OrgP transports.

352 **5.5 Internal nutrient sources and sinks**

353 The horizontal distributions of areas with internal sources and sinks of phosphorus and nitrogen are illustrated in
354 Fig. 8. A net inflow (inflow \geq outflow) of nutrients to each cell of the horizontal model grid is defined as a sink
355 (import) and counted as positive, while net outflow (inflow \leq outflow) is defined as a source (export) and counted
356 as negative (Eilola et al., 2012). Source areas of DIP generally coincide with sink areas of OrgP, and vice versa.

357 This is also partly true for DIN and OrgN, but the sink for DIN has a large contribution from denitrification that
358 transfers DIN to dissolved N₂. The difference between phosphorus and nitrogen sources and sinks is oxygen
359 dependent, because the removal of N is enhanced at lower oxygen concentrations, while the sediment phosphorus
360 sink is weakened (e.g., Savchuk, 2010). Sediments may even temporarily become a source under anoxic
361 conditions, when older mineral-bound P can be released to the overlying water. Source areas of DIN are mainly
362 found in the Gulf of Riga, and the deeper parts of the Arkona Basin and Bornholm Basin. The largest DIP sources
363 occur in the eastern parts of the Gotland Basin as well as in the deepest parts of the Bornholm Basin and Arkona
364 Basin, whereas the largest sink of OrgP occurs in the central Baltic proper. The main sources of DIP are generally
365 found in regions where water depth is greater than 70 m (in other words below the permanent halocline in the
366 Baltic proper), while the main sources of OrgP (and OrgN) are found in the productive coastal areas shallower
367 than about 30–40 m (see also Fig. 9). Indeed, DIP export is largest in areas with a water depth between 70 and
368 100 m, and decreases towards greater water depths (Fig. 9).

369
370 According to the accumulated import of nutrients (Fig. 9), the magnitude of the DIP export is larger than that
371 of the DIP import. This indicates that not all of the supply of phosphorus from land and atmosphere is retained
372 within the Baltic proper as will be further discussed from the nutrient budgets in section 5.6. For DIN, however,
373 we may notice only a very small net export from the Baltic proper to adjacent sub-basins, while for OrgP and
374 OrgN, imports and exports are almost balanced (Fig. 9). The nitrogen and phosphorus supply from land is
375 implemented in sea areas with a bottom depth usually of 6 m. This is where the river mouths are located in the
376 model.

377
378 There is a large import of DIP to areas with a depth range between 40–70 m (Fig. 9). This import does not
379 show a counter-part in the export of OrgP in Fig. 9. This result might be explained by local processes causing the
380 phytoplankton uptake and sediment deposition of DIP. There is an import of DIN to these areas that together with
381 nitrogen fixation and sediment–water fluxes of DIN may support local production of organic matter. The
382 phosphorus sink may be partly caused by oxygen dependent water–sediment fluxes that bind DIP to ironbound
383 phosphorus in oxic sediments (Almroth-Rosell et al., 2015). This effect is not included in Eilola et al. (2012), but
384 might potentially be accounted for by the adjusted DIP transports in REANA. The results of REANA indicate

385 that there is an additional sink but the relative importance of different processes causing this sink (data
386 assimilation or sediment processes) is, however, not possible to evaluate from the present reanalysis data set.

387

388 A partly opposite exchange profile is found for OrgP (Fig. 9). Coastal areas with a water depth of up to 40 m
389 are exporting organic phosphorus, whereas deeper areas import OrgP. Production in the coastal zone of the Baltic
390 proper and sedimentation in the open sea is almost balanced.

391

392 The largest export of DIN occurs due to rivers in the very shallow coastal zone. The magnitude of DIN imports
393 and exports in areas with greater water depths are much smaller. Obviously, DIN supplied from land is already
394 consumed in the coastal zone (Voss et al., 2005; Almroth-Rosell et al., 2011) and, consequently, only a minor
395 fraction of the nitrogen supplied to the shallow area can continuously reach regions deeper than 100 m (Eilola et
396 al., 2012; Radtke et al., 2012).

397 **5.6 Nutrient budgets of sub-basins**

398 The Baltic Sea is divided into seven sub-basins according to the selected sections, which form the borders of the
399 sub-basins (Fig. 1). We calculate total nutrient budgets for each of the sub-basins from the reanalysis (Figs. 10
400 and 11). Changes in pools are calculated as differences between 1971 and 1999 because the initial adjustment
401 process due to the assimilation is taking place during the first year (1970) (not shown). The largest annual mean
402 external phosphorus load occurs in the Baltic proper and amounts to 34.2 kton yr⁻¹ (Fig. 10). In addition, in the
403 Baltic proper the largest annual mean phosphorus sink of 25.0 kton yr⁻¹ is also found. Whereas during the period
404 1971–1999 the phosphorus content in the Gulf of Baltic proper increased, we found decreasing phosphorus
405 content in the Gulf of Finland, Bothnian Bay, Bothnian Sea and Danish Straits. Largest export and import of
406 phosphorus between sub-basins are found for the exchange between the Baltic proper and the Gulf of Finland,
407 which amount to 24.3 and 22.5 kton yr⁻¹, respectively. However, the largest net exchange (import minus export)
408 appears between the Baltic proper and Bothnian Sea. It is also found that the Baltic proper exports more
409 phosphorus to neighboring sub-basins than it imports, except for the Gulf of Riga. The annual mean net
410 phosphorus exported from the Baltic proper into the Danish Straits, the Bothnian Sea, the Gulf of Finland and
411 Gulf of Riga during the period 1971–1999 amounts to 1.7, 3.6, 1.8, and -0.6 kton yr⁻¹, respectively. The exchange

412 of phosphorus between the Baltic proper and the Gulf of Riga is smallest relative to the other three neighboring
413 sub-basins. Further, we found that the net transport, import and export of phosphorus into the Bothnian Bay are
414 smallest relative to the other sub-basins.

415

416 Nitrogen transports between Baltic Sea sub-basins are different compared to phosphorus transports (Fig. 11).
417 For example, the Baltic proper has larger nitrogen sinks than external sources. Further, during the period 1971–
418 1999 the nitrogen content decreased in the Gulf of Riga and increased in the Bothnian Bay, respectively. In the
419 Gulf of Finland and Danish Straits, the difference between external supply and internal sink of nitrogen is equal
420 to the net transport into the Gulf of Finland and Danish Straits. The large sink of nitrogen in the Bothnian Bay is
421 noteworthy. We also found relatively large net transports of nitrogen from the Gulf of Riga into the Baltic proper.
422 This is mainly explained by the relatively high nitrate concentrations in the Gulf of Riga relative to other sub-
423 basins.

424

425 The 3D nutrient pools constructed by data assimilation methods offer an opportunity to evaluate with improved
426 estimates the changes in Baltic Sea eutrophication. As an example, an investigation of the trophic state from
427 changes in five year average nutrient pools in REANA shows that the total nitrogen pool in the Baltic proper
428 increased from 657 kton to 1045 kton from the period 1971-1975 to 1995-1999 while the total phosphorus pool
429 decreased from 469 kton to 448 kton between the same periods. Hence, nitrogen increased by about 59% while
430 phosphorus decreased by about 4%. Similarly the pool of DIN in REANA increased by 80% while DIP decreased
431 by 6%. The corresponding numbers obtained from BED showed an increase of 100% for DIN and an increase of
432 7% of DIP. The results indicate large increases of nitrogen pools in the Baltic proper during the investigated
433 period but only relatively small changes of phosphorus pools.

434

435 Subsequent periodic assessments can be used to reveal future eutrophication changes. While estimating the
436 trophic state, it should be noticed that the change in trophic state depends on the chosen time periods. For
437 example, from the year 1971 to 1999 the total phosphorus (TP) in the Baltic proper increased with 2.7 kton yr^{-1} .
438 This result differs from the decrease seen from the five year average change discussed above. The reason is the
439 impact from short term fluctuations of nutrient content (Fig. 4) that may be larger than the long-term changes.

440

441

442 **5.7 Baltic nutrient flows**

443

444 To further analyze the variability of the budget of the reanalyzed nutrients, Fig. 12 provides the cross sectional,
445 integrated nutrient flows in the different sub-basins. Here the eastward and northward net transports are, by
446 definition, positive. Obviously, the integrated nutrient flows vary significantly in space according to the nutrient
447 loads from land. The inflows and outflows also vary depending on the depth of the water column and nutrient
448 concentrations that influence the vertically integrated mass fluxes. In general, the magnitude of nutrient transports
449 declines along transect A from south to north. For instance, the largest annual northward flow of nitrogen in the
450 Baltic proper reaches 392 kton yr^{-1} , while it is only 133 and 87 kton yr^{-1} for the Bothnian Sea and Bothnian Bay,
451 respectively.

452

453 In the Baltic proper, inflow and outflow as well as the net northward flow of phosphorus increase from the
454 south until a section along 56.8° N ; they remain then about constant until a section along 58.7° N , and thereafter
455 decrease rapidly further to the north. This indicates that major sources are located in the south where the large
456 rivers pour their loads into the Baltic Sea, while the major net sinks are mainly found in the northern parts of the
457 Baltic proper. The behavior of net northward flow of nitrogen is different. Nitrogen transports decrease
458 constantly with increasing latitude because the major sink works differently for nitrogen (i.e. denitrification) than
459 for phosphorus, which is retained mainly by burial in the sediments. The net northward flow decreases at the
460 latitude of the Gulf of Finland where phosphorus (and nitrogen) are transported towards the Gulf, as seen in
461 transect C.

462

463 In the Arkona and Bornholm basins, nitrogen and phosphorus transports increase from the west to the east. Due
464 to the nitrogen load from the Oder River, the inflow of nitrogen increases significantly at the border between the
465 Arkona and Bornholm basins, whereas the outflow does not show any discontinuity. As a result, the net flow of
466 nitrogen shows an accelerated increase. The situation for phosphorus in the Arkona and Bornholm basins is
467 different compared to the nitrogen transports because in- and outflow, as well as the net flow, change direction.
468 The phosphorus loads from the Oder River turn the outflow in the western parts into an inflow of phosphorus in
469 the eastern parts.

470

471 In the Gulf of Finland, in- and outflows generally decline from the west to east. In the entrance of the Gulf of
472 Finland, the net inflows of nutrients are almost zero. The largest net flow (westward) of nutrients appear at the
473 inner end of the Gulf of Finland, where the large river Neva enter the Gulf, with a magnitude of 33 kton yr⁻¹ for
474 nitrogen and 2.6 kton yr⁻¹ for phosphorus, respectively. The net flows of both phosphorus and nitrogen change
475 their directions in the Gulf of Finland and for nitrogen this change take place closer to the Baltic proper entrance
476 than for phosphorus. These results indicate that the large supply of nutrients from the Neva River are
477 accumulated or removed within the Gulf of Finland.

478 **6 Discussion**

479 **6.1 Biases of FREE**

480

481 RCO-SCOBİ has been widely used for the Baltic Sea and the model was carefully evaluated using various
482 observational data sets. As any other model, RCO-SCOBİ had to be calibrated because many processes including
483 sources and sinks of nutrients are known not in enough detail. Hence, an “optimal” parameterization of
484 unresolved processes is one of the requirements for the predictive capacity of the model. Further requirements to
485 calculate correct transports and transformation processes in addition to optimized model equations are high-
486 quality atmospheric and riverine forcing data, and high-quality initial and lateral boundary conditions.

487

488 Most of the large biases in FREE are caused by imperfect initial conditions. The reason is that the nutrient
489 pools in the sediments have not been spun up appropriately. As a consequence, phosphate concentrations in
490 FREE are higher than observed concentrations at all depths. The biases in surface phosphate concentrations
491 between model results and observations can influence the seasonal primary production. In REANA, however,
492 from the beginning of the experiment, the biases are already significantly reduced during the first year and remain
493 relatively small during the integration compared to FREE. This result indicates a need of new initial conditions of
494 the sediments.

495

496 **6.2 Non-conservation in REANA**

497

498 In the long-term simulation, the new initial condition for an assimilation cycle differs from the ending ocean state
499 of the last cycle when at that time observations are available. In this sense, the data assimilation introduces
500 sources and sinks of the nutrient cycles by interrupting the model simulation and adjusting the initial conditions.
501 The magnitudes of these artificial sources and sinks are directly related to the biases between model results and
502 observations. Figure 3 shows that the model has large biases during the beginning of the simulation. However,
503 data assimilation has corrected the mismatch between model state and observation to an “optimal” level during an
504 initial adjustment period. After the adjustment period, the mismatch between model and observation becomes
505 small and the successive adjustment due to data assimilation also becomes small. Further, the adjustment of data
506 assimilation is related to the spatial-temporal coverage of observations. Here we assimilated only observed
507 profiles into the model. After every assimilation cycle, the simulation continues with “optimal” initial conditions
508 based upon conservation principles. As the equations of RCO-SCBI have not been changed, masses of all
509 constituents of the model are conserved at least during the simulation between two assimilation occasions.

510

511 **6.3 Advantages of data assimilation**

512

513 The advantage of the data assimilation is that model variables at any station are very likely more accurate than
514 the model output without data assimilation. For instance, time series of profiles or transports across vertical
515 sections have very likely a smaller bias compared to observations than the corresponding model results without
516 data assimilation. Compared to available observations the information from the model is higher resolved and
517 homogeneous in space and time. Of course, it is difficult to evaluate the quality of model results at high
518 resolution because independent observational data sets are usually missing. An exceptional effort to utilize
519 independent data was done by Liu et al. (2014) showing that the statement about the added value of data
520 assimilation is true for one available, independent cruise data set at high resolution.

521

522 The results of the reanalysis can be used to estimate the water quality and ecological state with high spatial
523 and temporal resolution in regions and during periods when no measurements are available. This supports
524 improved assessments e.g. of eutrophication status indicators as exemplified in Section 5.6. Regional and local
525 model studies may use the data as initial and boundary conditions. For projections of future climate and for

526 nutrient load abatement scenario simulations the reanalysis has a very high scientific value as reference data set
527 for the historical period of the climate simulations. The evaluation of the regionalized climate (the statistics of
528 mesoscale variability, e.g. the mean state) during the historical period can be done much more accurate based
529 upon the reanalysis data than with sparse observational data. For instance, it is very difficult to calculate the
530 climatological mean state just from observations that are casted only during the ice-free season of the year. Using
531 a reanalysis as reference data for historical climate is a common method in regional climate studies of the
532 atmosphere. Here we provide a corresponding data set for the ocean to evaluate simulated present-day climate.
533

534 Further, nutrient transports across selected cross-sections or between vertical layers are calculated from the
535 reanalysis with high resolution and improved accuracy. However, one cannot expect that budgets calculated from
536 the summation of internal fluxes from model results with data assimilation are more accurate because usually
537 small artificial sources and sinks from the data assimilation are becoming as important as physically and
538 biogeochemically motivated sources and sinks when sums of fluxes are compared. Hence, we calculated in
539 Section 5.6 budgets only from external supply, imports and exports and changes in the water pools of nutrients
540 with the aim to compare the reanalysis results with other studies using only observations. It is perhaps not
541 possible to claim that our budgets are more accurate than budgets that are derived from observations only, despite
542 the higher temporal and spatial resolution in model outputs. However, the advantage of the reanalysis is that
543 measurements are extrapolated in space and time based upon physical principles of the model.
544

545 **6.4 Comparison with other assimilation methods**

546 Fu (2013) estimated the volume and salt transports during the 2003 MBI with a three-dimensional variational
547 data assimilation method (3DVAR) in the Baltic Sea. In the present study, we estimate the impact of the data
548 assimilation based upon the EnOI method on the net volume and nutrient transports as well as calculate budgets
549 for major sub-basins of the Baltic Sea. The volume transports obtained with different assimilation methods may
550 be different. The sea level in Fu (2013) is kept constant in the assimilation process, while sea level in this study is
551 varying accordingly during the assimilation of temperature and salinity based upon the statistical covariances.
552 The variability of sea level may enhance the barotropic flow, which is one of the reasons for the differences in net
553 volume transport between the results by Fu (2013) and REANA. However, transports within the sub-basin are
554 also indirectly affected by the interaction of baroclinicity and topography.

556 **6.5 Comparison with other studies on nutrient budgets**

557

558 In contrast to Eilola et al. (2012), in this study areas with DIN export are also found at the southern and eastern
559 coasts as well as at some small local regions in the inner parts of the Baltic proper (Fig. 8). In REANA, the
560 magnitudes of DIP imports and exports are larger than in Eilola et al. (2012), and there is pronounced import of
561 DIP in the western part of the Eastern Gotland Basin below 100 m (Fig. 8) that is not as significant in Eilola et al.
562 (2012). This, and the larger variability of DIN imports and exports, indicates that there is a higher degree of
563 small-scale localized transport and production patterns that are not captured by Eilola et al. (2012). Main sinks of
564 DIN are found in the deeper areas, but significant sinks are also seen in shallow areas and water depths of about
565 60m. As the assimilation of salinity observations result in a deeper halocline (Liu et al., 2014), the bottom water
566 in a depth range of 40–70 m contains higher oxygen concentrations than in the simulation without data
567 assimilation. Hence, in the REANA simulation of this study, more phosphorus is retained by the sediments in the
568 depth range of 40–70 m than in the simulation by Eilola et al. (2012). The present results show, however, an
569 export contribution from DIN sources in deeper areas (e.g. 60–90 m depths) that may have been caused by
570 reduced denitrification efficiency of oxidized sediments in the REANA simulation compared to Eilola et al.
571 (2012).

572

573 The in- and outflows of phosphorus between the sub-basins, except the Gulf of Riga and Gulf of Finland,
574 simulated in REANA are smaller than the results by Wulff and Stigebrandt (1989), Savchuk (2005) and Savchuk
575 and Wulff (2007). However, the net transports of phosphorus are similar between our results and these earlier
576 studies in all sub-basins. Moreover, the nitrogen budgets are much lower than the results of earlier studies,
577 especially in the Baltic proper. It should be kept in mind that the above mentioned studies estimated the nutrient
578 budgets from mass balance models together with inter-basin transport calculations based upon Knudsen's
579 formulae to calculate nutrient budgets of the Baltic Sea (see, e.g. Savchuk, 2005). Obviously, there are limitations
580 in calculations of previous studies. Despite overall uncertainties that also limit the reliability of our results, like
581 incomplete understanding of selected biogeochemical processes (e.g. nitrogen fixation), lacking information of
582 sediment parameters, and under-sampled observations in space and time, our approach has the advantage of using
583 both high-resolution modeling and all available observations made over a 30-year period. Our model results

584 consider the complete set of primitive equations in high-resolution, taking into account not only the volume and
585 salt conservation of sub-basins according to Knudsen's formulae, but also the wind-driven circulation between
586 and within sub-basins. Hence, we have, for the first time, the potential to quantify spatial transport patterns with
587 high confidence even within sub-basins, as in the exchange of nutrients between the coastal zone and the open
588 sea.

589

590 Eutrophication of the Baltic Sea is directly affected by the long-term evolution of external nutrient supply that
591 has three components (waterborne land loads, direct point sources at the coasts, and atmospheric depositions)
592 which are associated with the biogeochemical dynamics of the Baltic Sea. In our study, we used the reconstructed
593 external nutrient input data by Savchuk et al. (2012). Nutrient budgets (Figs. 10 and 11) of sub-basins are time-
594 averaged and represent in our study the overall results of the period 1970–1999. The phosphorus loads vary in
595 different periods, for example, the phosphorus loads in the 1980s are larger relative to the 1990s (see Savchuk et
596 al., 2012). Therefore, the phosphorus supply into the Gulf of Finland is greater in our study compared to Savchuk
597 and Wulff (2007). The greater phosphorus supply changes the phosphorus content and phosphorus concentration
598 in the Gulf of Finland. This is one reason why phosphorus transports between the Gulf of Finland and the Baltic
599 proper in our study are greater than the transports calculated by Savchuk (2005) and Savchuk and Wulff (2007).

600

601 Since our study covers a different time period compared to the studies by Wulff and Stigebrandt (1989),
602 Savchuk (2005) and Savchuk and Wulff (2007) nutrient concentrations and related budgets differ in time and
603 space. Hence, it is not surprising that other studies show deviating results. For example, during the period 1970–
604 1999, HELCOM (2013) showed that the TP concentration generally decreased in the Bothnian Bay and has
605 increased in the Gulf of Riga. However, these changes in TP concentrations were not monotonous. For example,
606 the TP concentration obviously increased during the period 1970–1976 in the Bothnian Bay. While in the
607 Bothnian Sea, TP concentration increased during the period 1970–1983 and decreased during the period 1990–
608 1999. Similarly, changes in total nitrogen concentration differed during different periods.

609

610 Gustafsson et al. (2012) used a process-oriented model that resolves the Baltic Sea spatially in 13 dynamically
611 interconnected and horizontally integrated sub-basins with high vertical resolution to reconstruct the temporal
612 evolution of eutrophication for 1850–2006. Savchuk (2005) and Savchuk and Wulff (2007) applied mass balance

613 models as mentioned above to calculate nutrient budgets of the Baltic Sea. The results of all these models depend
614 on the locations of the sub-basin borders which are chosen as far as possible according to dynamical constraints
615 such as sills or fronts that are parameterized to obtain estimates of the water exchanges. Using a high-resolution
616 circulation model, we showed that nutrient flows within the sub-basins may vary considerably (Fig. 12). For
617 instance, we found east- and westward net transports of nitrogen between the Baltic proper and Gulf of Finland
618 depending on border locations at 23.2° and 24.0° E, respectively. The importance of regional variations of sources
619 and sinks for nutrients on the calculation of transports between sub-basins therefore seems to be significant and
620 needs to be further studied. Given the uncertainty caused by data assimilation in the present study we must
621 however save the detailed studies of these issues to future work where the artificial impact of data assimilation on
622 sources and sinks will be traced and quantified during the run.

623 **7 Summary and Conclusion**

624 For the first time, a multi-decadal, high-resolution reanalysis of physical (temperature and salinity) and
625 biogeochemical variables (oxygen, nitrate, phosphate and ammonium) for the Baltic Sea was presented. The
626 reanalysis covers the period 1970–1999. A “weakly coupled” assimilation scheme using the EnOI method was
627 used to assimilate all available physical and biogeochemical observations into a high-resolution circulation model
628 of the Baltic Sea.

629

630 Both assimilated and independent observations collected from different databases were used to evaluate the
631 reanalysis results (REANA). Based on the model–data comparison presented in this study, we found that the
632 model results without data assimilation (FREE) exhibit significant biases in both oxygen and nutrients. The
633 reasons for these biases are not totally understood yet, although it is speculated that the main reasons might be
634 related to the imperfect initial conditions, limitations of model parameterizations, the inaccurate halocline
635 position and correspondingly the hypoxic volume (Liu et al. 2014). Based on the calculation of the overall RMSD
636 of oxygen and nutrient concentrations between model results and not-yet-assimilated observations, the results in
637 REANA are considerably better than those in FREE. The total RMSD of the oxygen, nitrate, phosphate and
638 ammonium is reduced respectively by 0.84 mL L⁻¹, 0.99 mmol m⁻³, 0.88 mmol m⁻³, 0.52 mmol m⁻³. This means

639 that the overall qualities of simulated oxygen, nitrate, phosphate, and ammonium concentrations are improved by
640 59, 46, 78 and 45%, respectively. These results demonstrate the strength of the applied assimilation scheme.

641
642 The observation information entering the model affects the oxygen dependent dynamics of biogeochemical
643 transports significantly due to both improved simulation of physical (e.g. vertical stratification) and
644 biogeochemical parameters (e.g. nutrient concentrations). As examples, we presented improved results of mean
645 seasonal cycles of nutrients, the spatial surface distributions of DIN, DIP and DIN:DIP of the entire Baltic Sea.

646
647 Based on the reanalysis simulation, we analyzed nutrient transports in the Baltic Sea. We found that vertically
648 integrated nutrient transports follow the general horizontal water circulation, and vary spatially to a large extent.
649 In particular, large nutrient transports were found in the Eastern Gotland Basin, in the Bornholm Basin, in the
650 Slupsk Channel and in the north-western Gotland Basin. The persistence of nutrient transports is greater in the
651 eastern and southern than in the northern and western Baltic Sea.

652
653 The horizontal distributions of sources and sinks of inorganic and organic nutrients show large spatial
654 variations and may be partly explained by (1) the external supply of nutrients from land, (2) the topographically
655 controlled horizontal nutrient exchange between sub-basins and between the coastal zone and the open sea, and
656 (3) vertical stratification that determines redox conditions at the sea floor. The latter is important for the
657 sediment-water fluxes of nutrients, and consequently for burial of nutrients in the sediments. The reanalysis
658 results suggest that in the Baltic proper, in most areas with a water depth less than the depth of the permanent
659 halocline at about 70–80 m, DIP is imported and transformed either to OrgP, or buried in the sediments in water
660 depths greater than the wave-induced zone at 40–70 m. Whether the latter is an artefact of the assimilation
661 method or a real sink is unclear. On the other hand, in areas with greater water depth, DIP is exported (e.g.
662 released from the sediments under anoxic conditions). Overall, the Baltic proper exports DIP to neighboring sub-
663 basins.

664
665 Nitrogen transports are very different compared to phosphorus transports. The shallow coastal zone with water
666 depths less than 10 m plays an outstanding role for DIN, because within it, large exports occur due to supplies
667 from land. The high productivity in the shallow areas effectively transfers DIN to OrgN and denitrification

668 decreases the exports of nitrogen from coastal areas to the deeper areas. Most of the exported DIN is removed in
669 shallow waters while at greater depths imports and exports of DIN are much smaller, indicating the important
670 role of the coastal zone for nitrogen removal.

671

672 Detailed nitrogen and phosphorus budgets suggest that nutrient transports in the various sub-basins are
673 controlled by different processes and show different response to external loads and internal sources and sinks. In
674 particular, the Baltic proper is the sub-basin with the largest nutrient exchanges with its surrounding sub-basins.
675 The Baltic proper exports phosphorus to all sub-basins except the Gulf of Riga. Similarly, the Baltic proper also
676 exports nitrogen to all sub-basins except to the Gulf of Riga and Danish Straits. In this sub-basin, also the largest
677 internal sink of all sub-basins was found. Noteworthy is the relatively large net export of phosphorus from the
678 Baltic proper into the Bothnian Sea. This finding is in agreement with previous studies. For the budgets of the
679 sub-basins, it is important where the borders of the sub-basins are located, because net transports may change
680 sign with the location of the border. For instance, in the entrance of the Gulf of Finland, the net phosphorus
681 transport from the Baltic proper is directed eastward, but changes direction at about 26°E. Further to the east, the
682 net phosphorus transport is directed westward.

683 **Acknowledgements**

684 The research presented in this study is part of the Baltic Earth programme (Earth System Science for the Baltic
685 Sea region, see <http://www.baltic.earth>), and was funded by the Swedish Research Council for Environment,
686 Agricultural Sciences and Spatial Planning (FORMAS) within the projects “Impact of accelerated future global
687 mean sea level rise on the phosphorus cycle in the Baltic Sea” (grant no. 214-2009-577), “Impact of changing
688 climate on circulation and biogeochemical cycles of the integrated North Sea and Baltic Sea system” (grant no.
689 214-2010-1575), and “Estimating nitrogen fixation in past and future climates of the Baltic Sea” (grant no. 214-
690 2013-1449), as well as by the Swedish Research Council within the project “Reconstructing and projecting Baltic
691 Sea climate variability 1850-2100” (grant no. 2012-2017). We thank Dr. Oleg Savchuk (Stockholm University)
692 and one anonymous reviewer for valuable comments that helped to improve the manuscript considerably.

693 **References**

694 Allen, J. I., Eknes, M., and Evensen, G.: An Ensemble Kalman Filter with a complex marine ecosystem model:

695 hindcasting phytoplankton in the Cretan Sea, *Ann. Geophys.*, 21, 399–411, doi:10.5194/angeo-21-399-2003,
696 2003.

697 Almroth-Rosell, E., Eilola, K., Hordoir, R., Meier, H.E.M., Hall, P.: Transport of fresh and resuspended
698 particulate organic material in the Baltic Sea — a model study, *J. Mar. Sys.* 87, 1–12, 2011.

699 Almroth-Rosell E., Eilola K., Kuznetsov I., Hall P., Meier H.E.M.: A new approach to model oxygen dependent
700 benthic phosphate fluxes in the Baltic Sea, *Journal of Marine Systems*, 144, 127–141, 2015.

701 Andersen, J. H., Carstensen, J., Conley, D. J., Dromph, K., Fleming-Lehtinen, V., Gustafsson, B. G., Josefson, A.
702 B., Norkko, A., Villnäs, A. and Murray, C.: Long-term temporal and spatial trends in eutrophication status of
703 the Baltic Sea. *Biological Reviews*. doi: 10.1111/brv.12221, 2015.

704 Beal, D., Brasseur, P., Brankart, J. M., Ourmieres, Y., and Verron, J.: Characterization of mixing errors in
705 a coupled physical biogeochemical model of the North Atlantic: implications for nonlinear estimation using
706 Gaussian anamorphosis, *Ocean Science*, 6, 247–262, 2010.

707 Beckmann, A., and Döscher, R.: A method for improved representation of dens water spreading over topography
708 in geopotential-coordinate models, *J. Phys. Oceanogr.*, 27, 581–591, 1997

709 Bengtsson, L., Hodges, K. and Hagemann, S.: Can Climate Trends be calculated from Re-Analysis Data?, *J.*
710 *Geophys. Res.*, 109, doi:10.1029/2004JD004536, 2004.

711 Bergström, S., and Carlsson, B.: River runoff to the Baltic Sea: 1950–1990, *Ambio*, 23, 280–287, 1994.

712 Boesch, D., Hecky, R., O’Melia, C., Schindler, D., and Seitzinger, S.: Eutrophication of seas along Sweden’s
713 West Coast. Report No. 5898. Swedish Environmental Protection Agency. P 78, 2008

714 Carton, J.A., Giese, B.S., and Grodsky, S.A.: Sea level rise and the warming of the oceans in the SODA ocean
715 reanalysis, *J. Geophys. Res.*, 110, 10.1029/2004JC002817, 2005.

716 Ciavatta, S., Kay, S., Saux-Picart, S., Butenschön, M. and Allen, J. I.: Decadal reanalysis of biogeochemical
717 indicators and fluxes in the North West European shelf-sea ecosystem, *J. Geophys. Res. Oceans*, 121, 1824–
718 1845, 2016. Claustre H., Antoine D., Boehme L., Boss E., D’Ortenzio F., Fanton D’Andon, O., Guinet, C.,
719 Gruber, N., Handegard, N.O., Hood, M., Johnson, K., Körtzinger, A., Lampitt, R., LeTraon, P.-Y., Lequéré,
720 C., Lewis, M., Perry, M.-J., Platt, T., Roemmich, D., Sathyendranath, S., Testor, P., Send, U. and Yoder, J.:
721 Guidelines Towards an Integrated Ocean Observation System for Ecosystems and Biogeochemical Cycles,
722 Proceedings of OceanObs’09: Sustained Ocean Observations and Information for Society (Vol. 1), Venice,
723 Italy, 21–25 September 2009, edited by: Hall, J., Harrison, D. E., and Stammer, D., ESA Publication WPP-

724 306, doi:10.5270/OceanObs09.pp.14, 2010.

- 725 Conley, D.J., Björck, S., Bonsdorff, E., Carstensen, J., Destouni, G., Gustafsson, B.G., Hietanen, S., Kortekaas,
726 M., Kuosa, H., Meier, H.E.M., Müller-Karulis, B., Nordberg, K., Norkko, A., Nürnberg, G., Pitkänen, H.,
727 Rabalais, N.N., Rosenberg, R., Savchuk, O.P., Slomp, C.P., Voss, M., Wulff, F., Zillén, L.: Hypoxia-related
728 processes in the Baltic Sea. Critical review. Environ. Sci. Technol. 43 (10), 3412–3420, 2009.
- 729 Daewel, U., and Schrum, C.: Simulating long-term dynamics of the coupled North Sea and Baltic Sea ecosystem
730 with ECOSMO II: model description and validation, J. Mar. Syst., 119–120, 30–49, 2013.
- 731 Eilola, K., Almroth-Rosell, E., Dieterich, C., Fransner, F., Höglund, A., and Meier, H.E.M.: Modeling nutrient
732 transports and exchanges of nutrients between shallow regions and the open Baltic Sea in present and future
733 climate, Ambio., 41, 574–585, 2012.
- 734 Eilola, K., Almroth-Rosell, E., and Meier, H.E.M.: Impact of saltwater inflows on phosphorus cycling and
735 eutrophication in the Baltic Sea. A 3D model study. Tellus A, 66, 23985, DOI: 10.3402/tellusa.v66.23985,
736 2014.
- 737 Eilola, K., Gustafson, B.G., Kuznetsov, I., Meier, H.E.M., Neumann, T., and Savchuk, O.P.: Evaluation of
738 biogeochemical cycles in an ensemble of three state-of-the-art numerical models of the Baltic Sea, J. Mar.
739 Syst., 88, 267–284, 2011.
- 740 Eilola, K., Meier, H. E. M., and Almroth, E.: On the dynamics of oxygen, phosphorus and cyanobacteria in the
741 Baltic Sea: a model study, J. Mar. Syst., 75, 163–184, 2009.
- 742 Eilola, K., Mårtensson, S., and Meier, H. E. M.: Modeling the impact of reduced sea ice cover in future climate
743 on the Baltic Sea biogeochemistry, Geophys. Res. Lett., 40, 1–6, 2013.
- 744 Fischer, H., and Matthäus, W.: The importance of the Drogden Sill in the Sound for major Baltic inflows, J. Mar.
745 Syst., 9, 137–157, 1996.
- 746 Fontana C., Brasseur, P., and Brankart, J.-M.: Toward a multivariate reanalysis of the North Atlantic Ocean
747 biogeochemistry during 1998–2006 based on the assimilation of SeaWiFS chlorophyll data, Ocean Sci., 9,
748 37–56, 2013.
- 749 Friedrichs, M.A.M., Hood, R., and Wiggert, J.: Ecosystem model complexity versus physical forcing: Quantifi-
750 cation of their relative impact with assimilated Arabian Sea data, Deep-Sea Res. II, 53, 576–600, 2006.
- 751 Fu, W.: Estimating the volume and salt transports during a major inflow event in the Baltic Sea with the
752 reanalysis of the hydrography based on 3DVAR. J. Geophys. Res. Oceans, 118, 3103–3113. 2013.

- 753 Fu, W., She J., and Dobrynin, M.: A 20-year reanalysis experiment in the Baltic Sea using three-dimensional
754 variational (3DVAR) method. *Ocean Sci.*, 8(5), 827–844, 2012.
- 755 Fu, W.: On the role of temperature and salinity data assimilation to constrain a coupled physical-biogeochemical
756 model in the Baltic Sea. *J. Phys. Oceanogr.*, 46, 713–729, 2016.
- 757 Gerdes, R., Köberle, C., and Willebrand, J.: The influence of numerical advection schemes on the results of
758 ocean general circulation models, *Climate Dyn.*, 5, 211–226, 1991.
- 759 Gregg, W.W., Friedrichs, M.A.M., Robinson, A. R., Rose, K. A., Schlitzer, R., Thompson, K. R., and Doney,
760 S.C.: Skill assessment in ocean biological data assimilation, *J. Marine Syst.*, 76, 16–33, 2009.
- 761 Gustafsson, B.G., Schenk, F., Blenckner, T., Eilola, K., Meier, H.E.M., Müller-Karulis, B., Neumann, T., Ruoho-
762 Airola, T., Savchuk, O.P., and Zorita, E.: Reconstructing the Development of Baltic Sea Eutrophication
763 1850–2006. *AMBIO*, 41, 534–548, 2012.
- 764 HELCOM: Approaches and methods for eutrophication target setting in the Baltic Sea region. *Balt. Sea Environ.*
765 *Proc. No. 133*, 2013.
- 766 Hibler, W. D. : A dynamic thermodynamic sea ice model, *J. Phys.Oceanogr.*, 9, 817–846, 1979.
- 767 Hoteit, I., Triantafyllou, G., and Petihakis, G.: Efficient data assimilation into a complex, 3-D physical-
768 biogeochemical model using partially-local Kalman filters, *Ann. Geophys.*, 23, 3171–3185, 2005.
- 769 Hoteit, I., Triantafyllou, G., Petihakis, G., and Allen, J. I.: A singular evolutive extended Kalman filter to
770 assimilate real in situ data in a 1-D marine ecosystem model, *Ann. Geophys.*, 21, 389–397, 2003.
- 771 Hunke, E.C., and Dukowicz J.K.: An elastic-viscous-plastic model for sea ice dynamics, *J. Phys. Oceanogr.*, 27,
772 1849–1867, 1997.
- 773 Killworth, P.D., Stainforth, D., Webb, D.J., and Paterson S. M.: The development of a free-surface Bryan-Cox-
774 Semtner ocean model, *J. Phys. Oceanogr.*, 21, 1333–1348, 1991.
- 775 Lass, H.-U., Prandke, H., and Liljebladh, B.: Dissipation in the Baltic Proper during winter stratification, *J.*
776 *Geophys. Res.*, 108, 3187, doi:10.1029/72002JC001401, 2003.
- 777 Liu, Y., Meier, H. E. M., and Axell, L.: Reanalyzing temperature and salinity on decadal time scales using the
778 ensemble optimal interpolation data assimilation method and a 3-D ocean circulation model of the Baltic
779 Sea, *J. Geophys. Res. Oceans.*, 118, 5536–5554, 2013.
- 780 Liu Y., Meier, H.E.M., and Eilola, K.: Improving the multiannual, high-resolution modelling of biogeochemical
781 cycles in the Baltic Sea by using data assimilation, *Tellus A*, 66, 24908,

782 <http://dx.doi.org/10.3402/tellusa.v66.24908>, 2014.

- 783 Maar, M., Møller, E. F., Larsen, J., Madsen, K. S., Wan, Z., She, J., Jonasson, L., and Neumann, T.: Ecosystem
784 modelling across a salinity gradient from the North Sea to the Baltic Sea, *Ecol. Model*, 222, 1696–1711,
785 2011.
- 786 Marmefelt, E., Arheimer, B., and Langner, J.: An integrated biochemical model system for the Baltic Sea.
787 *Hydrobiologia* 393, 45–56, 1999.
- 788 Matthäus, W., and Franck, H.: Characteristics of major Baltic inflows—A statistical analysis, *Cont. Shelf Res.*,
789 12, 1375–1400, 1992.
- 790 Meier, H. E. M.: On the parameterization of mixing in three-dimensional Baltic Sea models, *J. Geophys. Res.*,
791 106, 30997–31016, 2001.
- 792 Meier, H. E. M.: Modeling the pathways and ages of inflowing salt and freshwater in the Baltic Sea, *Estuar.
793 Coast. Shelf Sci.*, 74, 610–627, 2007.
- 794 Meier, H.E.M., and Kauker, F.: Sensitivity of the Baltic Sea salinity to the freshwater supply. *Clim. Res.*, 24,
795 231-242, 2003.
- 796 Meier, H.E.M., Andersson, H.C., Dieterich, C., Eilola, K., Gustafsson, B.G., Höglund, A., and Schimanke, S.:
797 Modeling the combined impact of changing climate and changing socio-economic development on the Baltic
798 Sea environment in an ensemble of transient simulations for 1961-2099. *Clim. Dynam.*, 39, 2421-2441,
799 2012.
- 800 Meier, H.E.M., Andersson, H.C., Eilola K., Gustafsson B.G., Kuznetsov I., Müller-Karulis, B., Neumann T., and
801 Savchuk, O.P.: Hypoxia in future climates: A model ensemble study for the Baltic Sea. *Geophys. Res. Lett.*,
802 38, L24608, 2011.
- 803 Meier, H.E.M., Döscher, R., and Faxen, T.: A multiprocessor coupled ice-ocean model for the Baltic Sea:
804 Application to the salt inflow, *J. Geophys. Res.*, 108(C8), 3273. doi:10.1029/2000JC000521, 2003.
- 805 Natvik, L.-J., and Evensen, G.: Assimilation of ocean colour data into a biochemical model of the North Atlantic
806 – Part 1: Data assimilation experiments, *J. Marine Syst.*, 40–41, 127–153, 2003.
- 807 Neumann, T., Fennel, W., and Kremp, C.: Experimental simulations with an ecosystem model of the Baltic Sea.
808 *Global Biogeochemical Cycles* 16 (3), 1–19, 2002.
- 809 Orlanski, I.: A simple boundary condition for unbounded hyperbolic flows, *J. Comput. Phys.*, 21, 251–269, 1976.
- 810 Pawlak, J.F., Laamanen, M., and Andersen, J.H.: Eutrophication in the Baltic Sea-an integrated thematic

811 assessment of the effects of nutrient enrichment in the Baltic Sea Region. An executive summary. Baltic Sea
812 Environment Proceedings No. 115A. Helsinki Commission (Baltic Marine Environment Protection
813 Commission), p. 18. pp., 2009.

814 Radtke, H., Neumann, T., Voss, M., and Fennel, W.: Modeling pathways of riverine nitrogen and phosphorus in
815 the Baltic Sea. *J. Geophys. Res. Oceans* (1978-2012) 117(C9), C09024, 2012.

816 Samuelsson, P., Jones, C. G., Willn, U., Ullerstig, A., Golvik, S., Hansson, U., Jansson, C., Kjellström, E.,
817 Nikulin, G., and Wyser, K.: The Rossby Centre Regional Climate model RCA3: model description and
818 performance. *Tellus A*, 63, 4–23, 2011.

819 Savchuk, O.P.: Resolving the Baltic Sea into seven subbasins: N and P budgets for 1991–1999. *Journal of Marine*
820 *Systems*, 56, 1–15, 2005.

821 Savchuk, O.P.: Large-scale dynamics of hypoxia in the Baltic Sea. In *Chemical structure of pelagic redox*
822 *interfaces: observation and modelling*, ed. E.V. Yakushev. Handbook of environmental chemistry, 24 pp.
823 Berlin: Springer. doi:10.1007/698_2010_53, 2010.

824 Savchuk, O.P., and Wulff, F.: Modeling the Baltic Sea Eutrophication in a Decision Support System. *Ambio* , 36,
825 2–3, 2007.

826 Savchuk, O.P., Gustafsson, B. G., Rodriguez Medina, M., Sokolov, A.V., and Wulff, F.V.: Nutrient Loads to the
827 Baltic Sea. 1970-2006, Technical Report, No. 5. Baltic Nest Institute, Stockholm, Sweden, 2012.

828 She, J., Høyer, J.L., and Larsen, J.: Assessment of sea surface temperature observational networks in the Baltic
829 Sea and North Sea. *Journal of Marine systems*, 65, 314–335, 2007.

830 Sokolov, A., Andrejev O., Wulff, F., and Rodriguez Medina, M.: The Data Assimilation System for Data
831 Analysis in the Baltic Sea. *Systems Ecology Contributions*, 3, Stockholm University, 1997, 66pp.

832 Stevens, D. P.: The open boundary conditions in the United Kingdom fine-resolution Antarctic model, *J. Phys.*
833 *Oceanogr.*, 21, 1494–1499, 1991.

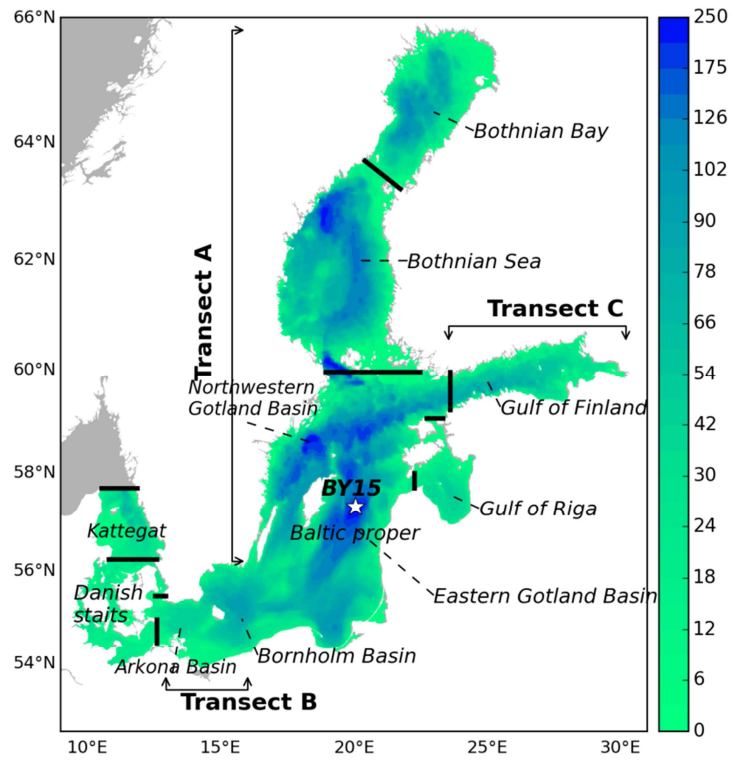
834 Teruzzi, A., Dobricic, S., Solidoro, C., and Cossarini, G.: A 3-D variational assimilation scheme in coupled
835 transport-biogeochemical models: Forecast of Mediterranean biogeochemical properties, *J. Geophys. Res.*
836 *Oceans*, 119, 200-217, 2014.

837 Triantafyllou, G., Korres, G., Hoteit, I., Petihakis, G., and Banks, A.C.: Assimilation of ocean colour data into a
838 Biogeochemical Flux Model of the Eastern Mediterranean Sea *Ocean Sci.*, 3, 397–410, 2007.

839 Triantafyllou, G., Hoteit, I., Luo, X., Tsiaras, K., and Petihakis, G.: Assessing a robust ensemble-based Kalman

- 840 filter for efficient ecosystem data assimilation of the Cretan Sea, *Journal of Marine Systems*, 125, 90–100,
841 2013.
- 842 Väli, G., Meier, H.E.M., and Elken, J.: Simulated halocline variability in the Baltic Sea and its impact on hypoxia
843 during 1961-2007, *J. Geophys. Res. Oceans*, 118, 6982-7000, doi:10.1002/2013JC009192, 2013.
- 844 Voss, M., Emeis, K.-C., Hille, S., Neumann, T., and Dippner, J.W.: Nitrogen cycle of the Baltic Sea from an
845 isotopic perspective. *Global Biogeochemical Cycles* 19: GB3001. doi: 10.1029/2004GB002338, 2005.
- 846 While, J., Totterdell, I., and Martin, M.: Assimilation of pCO₂ data into a global coupled physical-
847 biogeochemical ocean model, *J. Geophys. Res.*, 117, C03037, doi:10.1029/2010JC006815, 2012.
- 848 Wulff, F., Rahm, L., Larsson, P. (Eds.): *A systems analysis of the Baltic Sea: Ecological Studies, Vol. 148.*
849 Springer, Berlin, 2001.
- Wulff, F., and Stigebrandt, A.: A time-dependent budget model for nutrients in the Baltic Sea. *Global
Biogeochemical Cycles*, 3(1), 63–78, 1989.

850
851
852

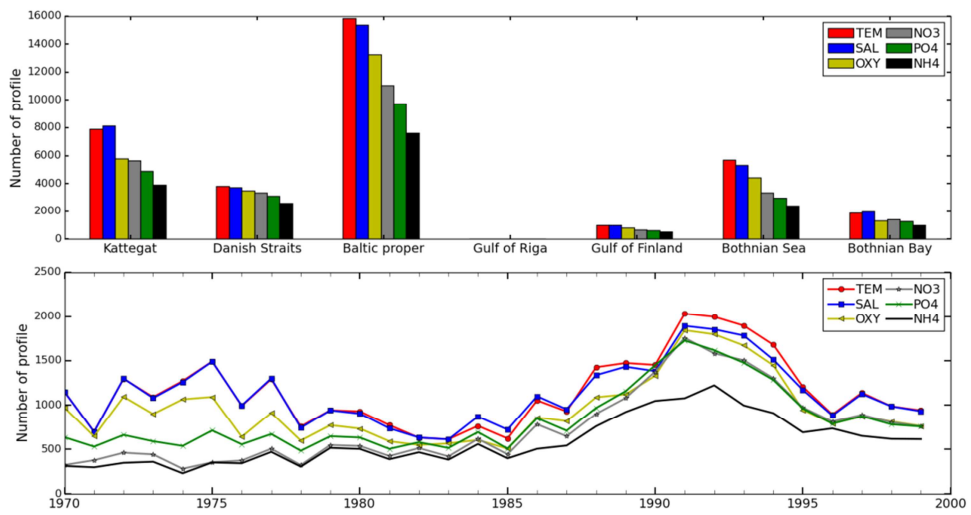


853

854 Figure 1. The bathymetry of the model (depth in m). The border locations of sub-basins of the Baltic Sea used in
 855 this study are shown by the black lines, and the BY15 station is shown by the white star. Names of the sub-basins
 856 are the Kattegat (KT), Danish Straits (DS), the Baltic proper (BP), the Gulf of Riga (GR), the Gulf of Finland
 857 (GF), the Bothnian Sea (BS), and the Bothnian Bay (BB).

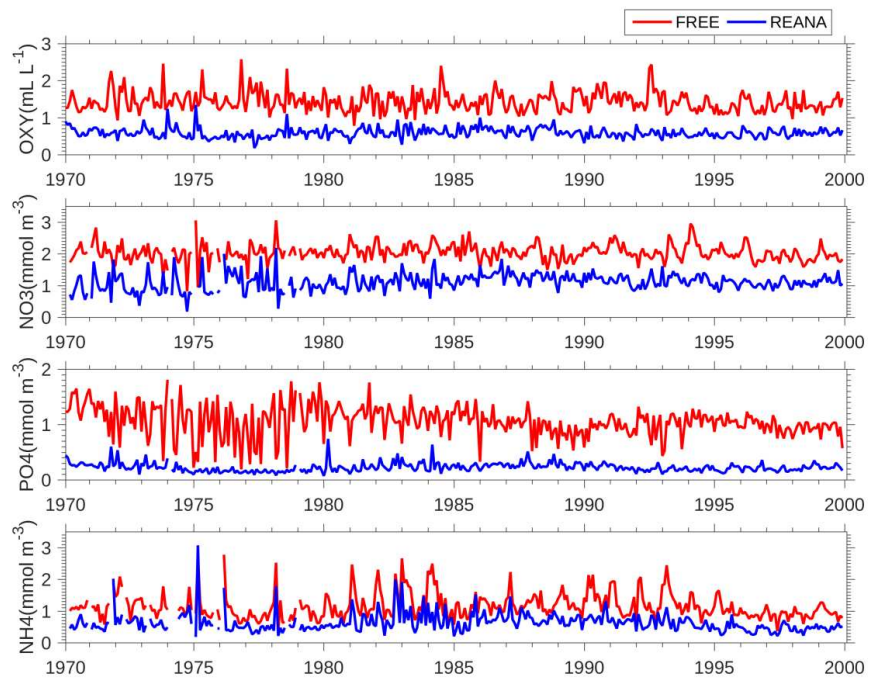
858

859
860
861



862

863 Figure 2. Number of observed profiles in different sub-basins (upper panel) and annual number of profiles from
864 1970–1999 (bottom panel).



866

867 Figure 3. Monthly mean root mean square deviation (RMSD) between model results and observations for
868 oxygen, nitrate, phosphate and ammonium in FREE (red) and REANA (blue).

869

870

871

872

873

874

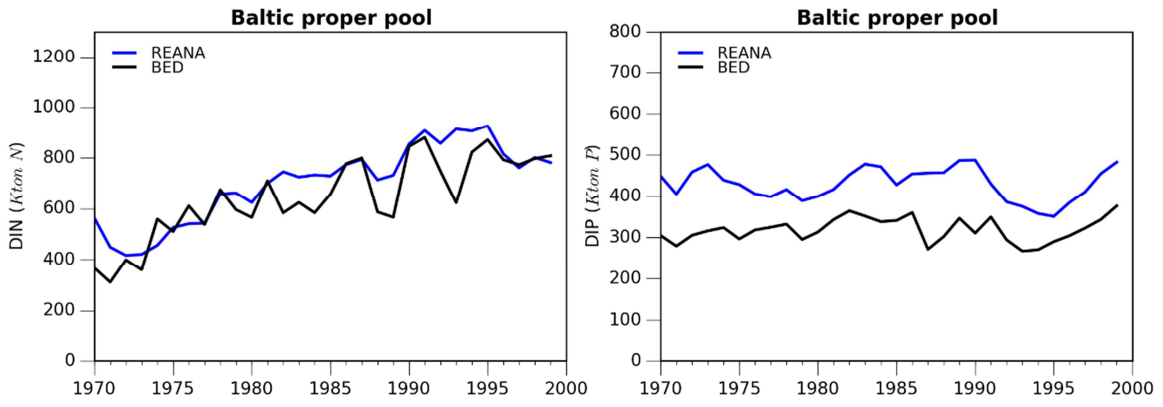
875

876

877

878

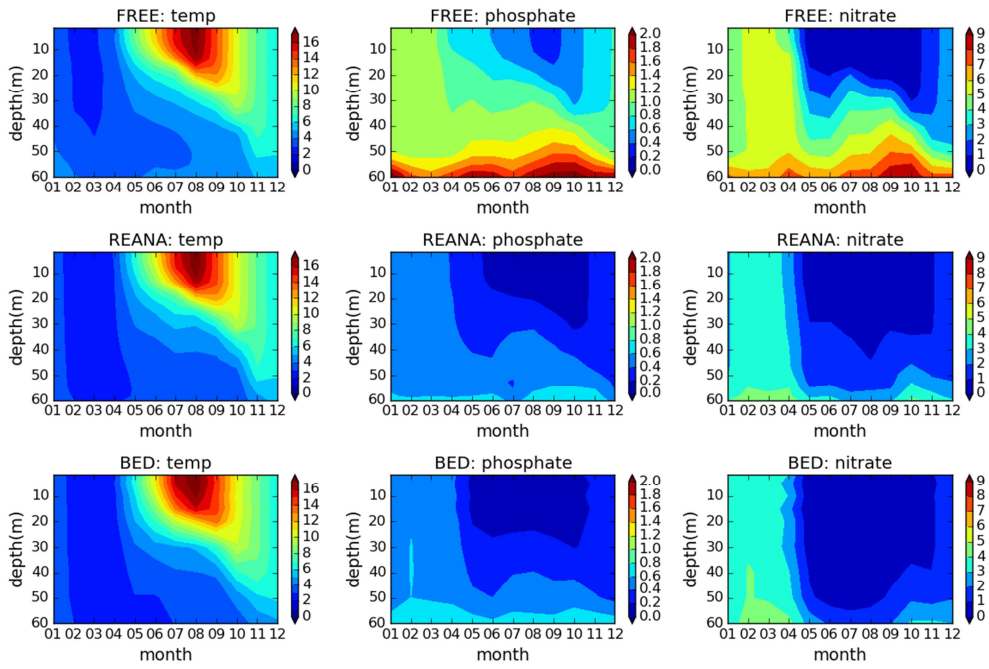
879



880

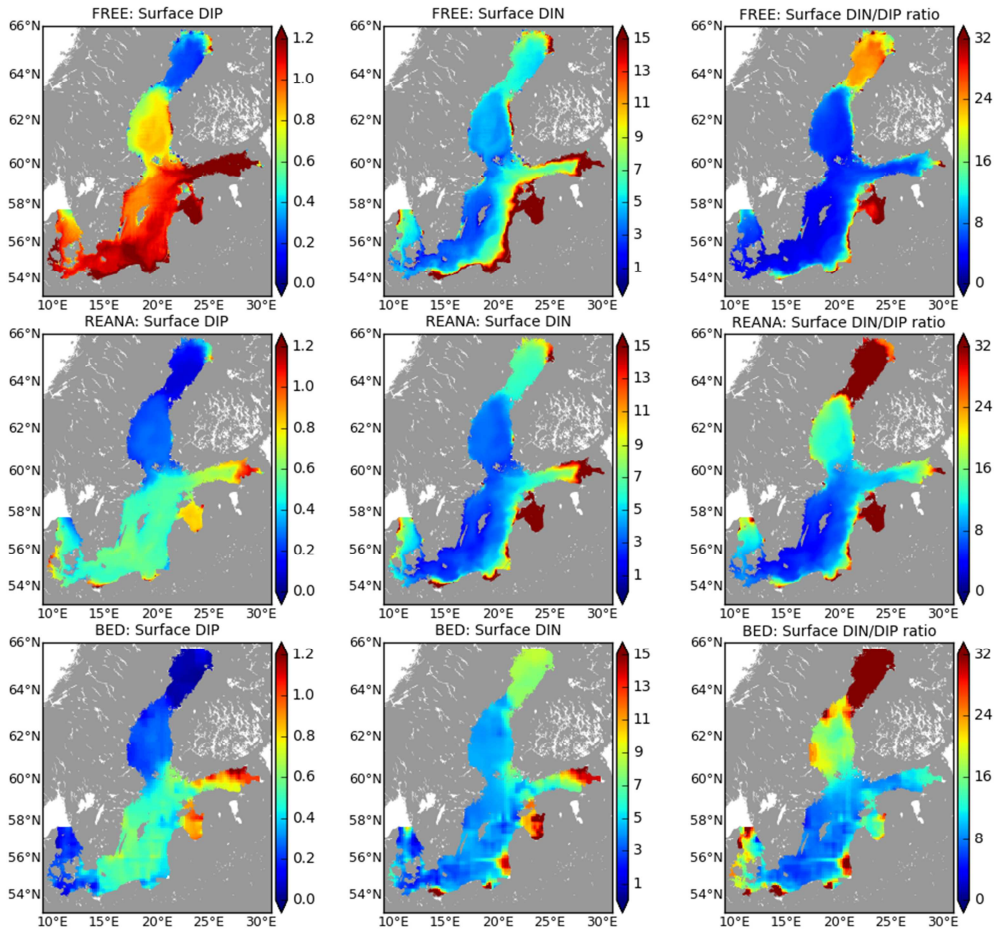
881

882 Figure 4. Annual mean integrated pools (in kton) of pelagic DIN and DIP in the Baltic proper calculated from
 883 REANA and from observations in BED.



884

885 Figure 5. The seasonal cycle of monthly average (1970–1999) temperature ($^{\circ}\text{C}$), phosphate concentration (mmol
 886 m^{-3}), and nitrate concentration (mmol m^{-3}) at BY15 for FREE (row 1), REANA (row 2), and BED data (row 3),
 887 respectively.

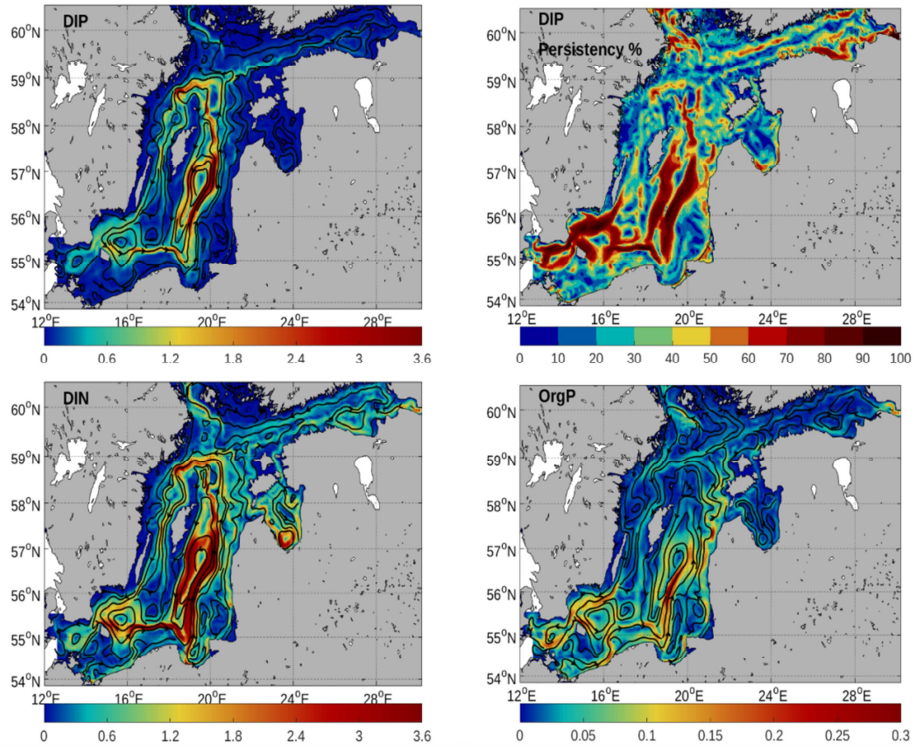


888

889 Figure 6. Simulated monthly (March) mean (1970–1999) surface layer (0–10 m) concentrations of DIP (mmol m^{-3}) (left), DIN (mmol m^{-3}) (middle), and the corresponding DIN to DIP ratio (right) from FREE and REANA are
 890
 891 shown in rows 1 and 2, respectively. The corresponding BED maps in row 3 are calculated from observations
 892 monitored during the period 1995-2005.

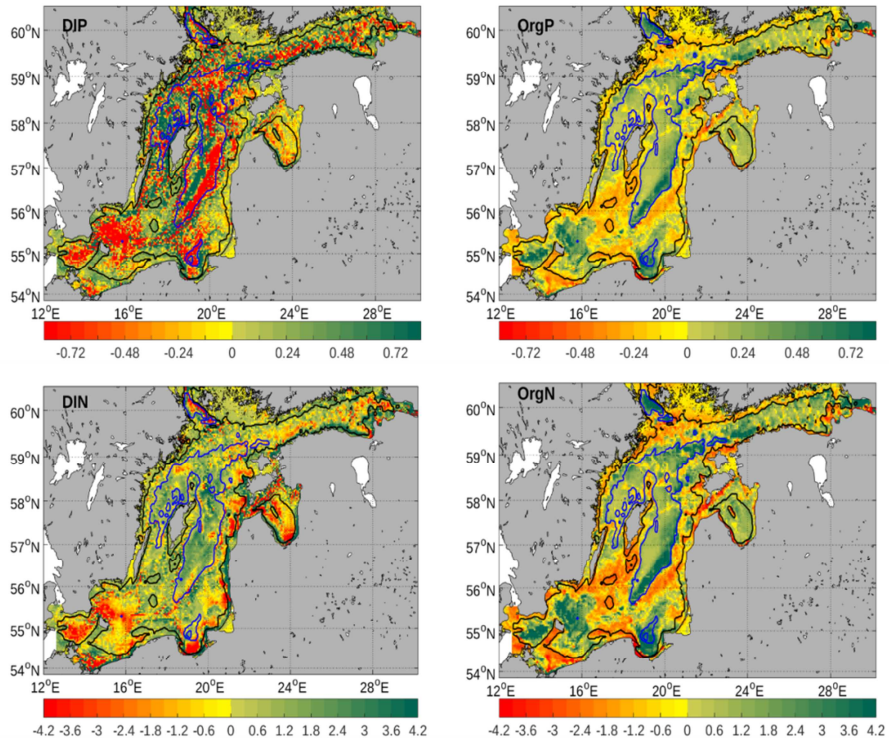
893

894



895 Figure 7. Annual mean DIP transports and the corresponding DIP persistency, DIN and OrgP transports for
896 REANA averaged for the period 1970–1999. The black solid lines with arrows show the streamlines and
897 direction of transports. The magnitude of transports (kton km⁻¹ yr⁻¹) and the persistency (%) are shown by the
898 background color. The corresponding values are shown in the colored bars.

899



900
901
902
903
904
905

Figure 8. Spatial distributions of annual mean import of DIP, OrgP, DIN and OrgN averaged for the period 1970–1999. The magnitude of import and its corresponding value ($\text{kton km}^{-2} \text{yr}^{-1}$) are shown by the background color and color bar, respectively. Green colors denote positive values (import), and yellow to red colors denote negative values (export). The black and blue lines show 30 and 100 m depth contours of the model, respectively.

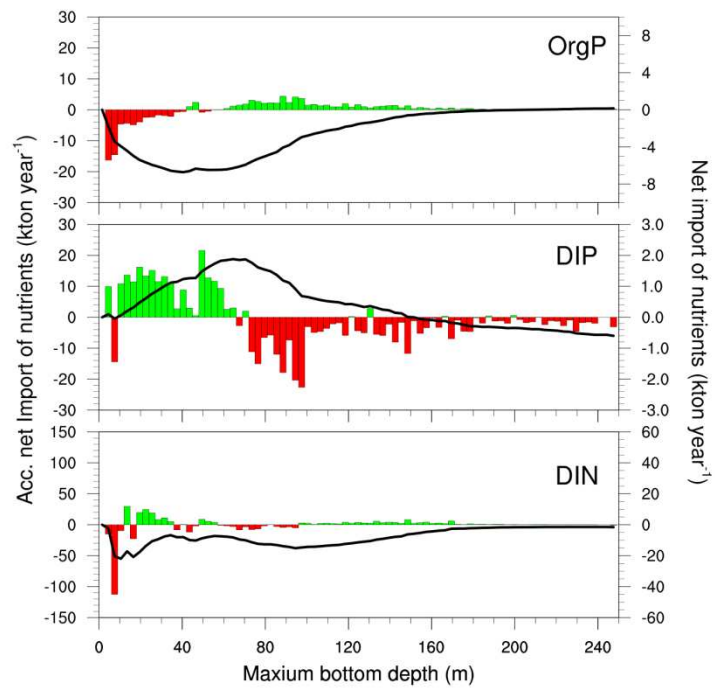
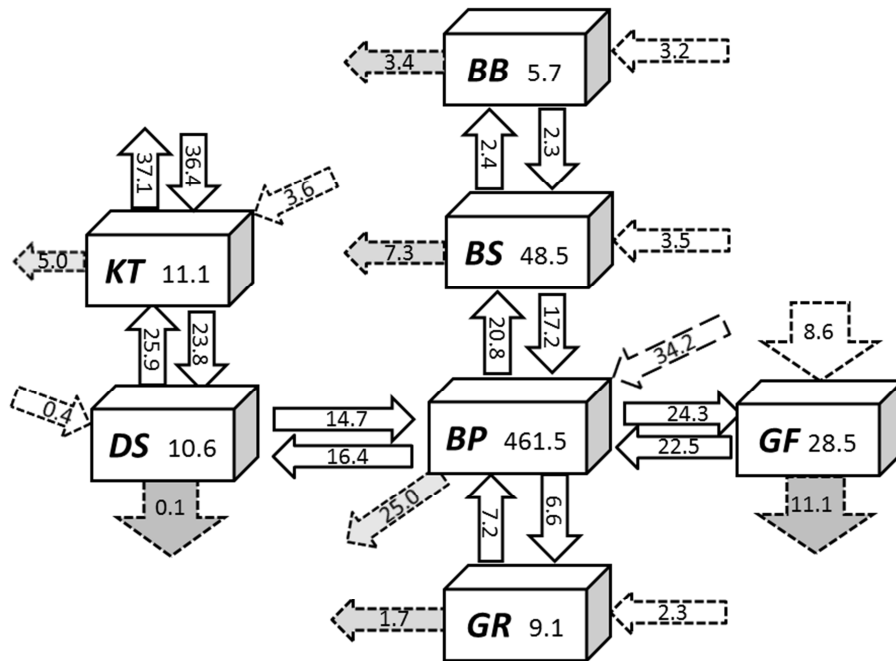


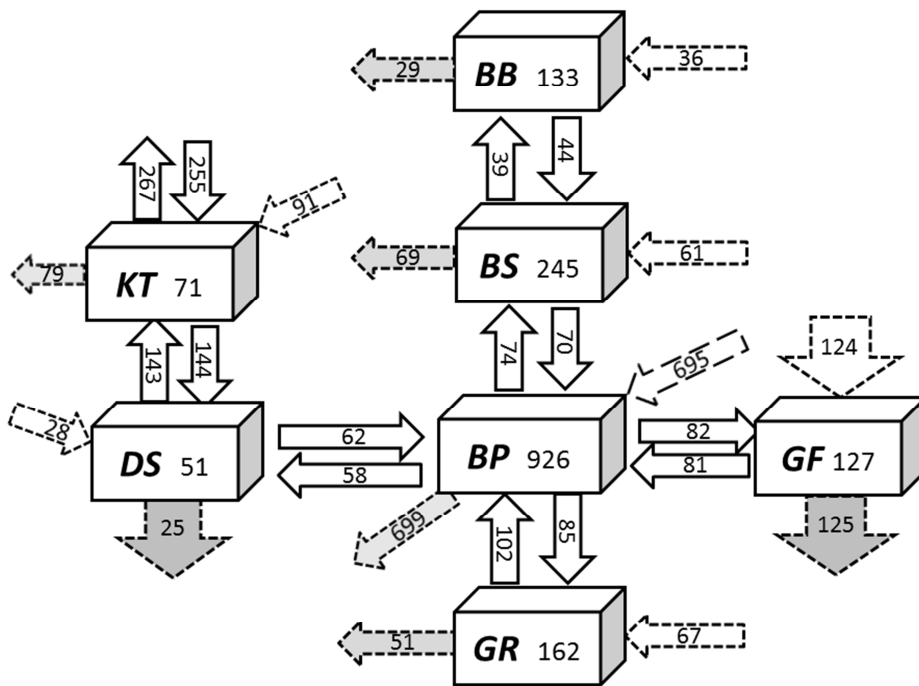
Figure 9. Annual mean, accumulated net imports (black lines) and imports of OrgP, DIP and DIN (color bars) to regions with the same depth in the Baltic proper averaged for the period 1970–1999.



907

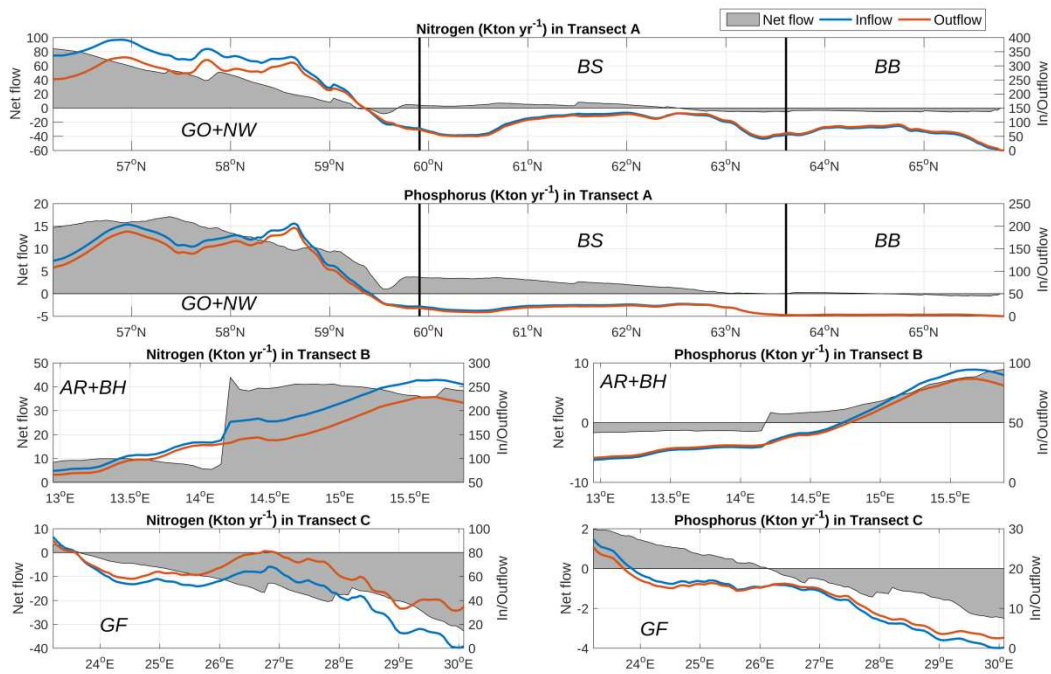
908 Figure 10. Annual mean total phosphorus budgets of the Baltic Sea averaged for the period 1971–1999. The
 909 average total amounts are in kton, and transport flows and sink/source fluxes (external nutrient inputs/sink) are in
 910 kton yr⁻¹. External nutrient inputs from atmosphere and land are combined.

911



912

913 Figure 11. The same as Figure 9, but for nitrogen.



914

915 Figure 12. Annual mean fluxes of nitrogen (in kton yr^{-1}) and phosphorus (in kton yr^{-1}) as a function of the cross
 916 sections along transects following the latitude and longitude in the Baltic sub-basins. Northward and eastward
 917 fluxes are, by definition, positive and called inflows. Southward and westward flows are called outflows. Net
 918 flow is the difference between in- and outflows. Here, AR, BH, GO, NW, GF, BS, and BB represent the Arkona
 919 Sea, Bornholm Sea, Eastern Gotland Basin, Northwestern Gotland Basin, Gulf of Finland, Bothnian Sea and
 920 Bothnian Bay, respectively. Transect A summarizes fluxes from the southern Baltic proper to the Bothnian Bay.
 921 Transect B describes the Baltic Sea entrance area from the Arkona Basin to the Bornholm Basin, and transect C
 922 summarizes fluxes in the Gulf of Finland (see Fig. 1).